This is to certify that the
thesis entitled

A TOPCOLOR MODEL WITH FLAVOR-UNIVERSAL
HYPERCHARGE SECTOR

presented by

FELIX BRAAM

has been accepted towards fulfillment
of the requirements for the

M.S. degree in PHYSICS AND ASTRONOMY

Elizabeth H. Simmons
Major Professor's Signature

June 29, 2007
Date

A TOPCOLOR MODEL WITH FLAVOR-UNIVERSAL HYPERCHARGE SECTOR

By

Felix Braam

A THESIS

Submitted to
Michigan State University
in partial fulfillment of the requirements
for the degree of

MASTER of Science

Department of Physics and Astronomy

2007

ABSTRACT

A TOPCOLOR MODEL WITH FLAVOR-UNIVERSAL HYPERCHARGE SECTOR

By

Felix Braam

The standard model of the electroweak interactions, including electroweak symmetry breaking and the fermion masses, is in good agreement with most of the current data. Nevertheless its key ingredient, the "Higgs"-particle, is not completely satisfactory. Technicolor models have been able to give an alternative explanation of the symmetry breaking pattern. In order to explain the origin of fermion masses technicolor has been embedded in a larger model, called "extended" technicolor. The large mass of the top quark further suggests the existence of new dynamics called "topcolor" associated with the third generation of fermions.

The subject of this thesis is a topcolor model that by assuming an additional strong gauge interaction coupling only to the third quark generation explains the large top mass. Unlike previously discussed topcolor models, this model does not distinguish between the third and the first, and second generation of fermions in the hypercharge sector. Implications from current experimental data are discussed.

ACKNOWLEDGMENTS

I especially would like to thank my advisors Prof. R. Sekhar Chivukula, and Prof. Elizabeth H. Simmons and my fellow student Michael Floßdorf. Further, I would like to mention Dr. Kazuhiro Tobe and Baradhwaj Coleppa who helped me during various long discussions.

TABLE OF CONTENTS

LIST OF TABLES

LIST OF FIGURES

Chapter 1

Introduction

The standard model provides a theory which is able to explain the currently observed physics, including the heavy gauge boson and fermion masses, very accurately. Nevertheless, there are several indications ("fine-tuning", etc.), associated with the Higgs-particle which drives the electroweak symmetry breaking, that suggest that the standard model should be regarded as effective theory up to the TeV-scale. Technicolor models [10] can give an alternative, dynamical, explanation of the symmetry breaking pattern, yielding correct predictions for the heavy gauge boson masses. In order to explain the origin of the fermion masses technicolor has been embedded into a larger model, called "extended" technicolor [10]. The discovery of the large top mass led to complications that could not be compensated within extended technicolor. Topcolor models [11] associate new dynamics with the third generation of fermions in order to create the large top mass.

The subject of this thesis is a topcolor model with a flavor universal hypercharge sector.

In order to give a picture of the framework in which this model has to be seen and to establish the necessary terminology, we shall briefly review the relevant parts of modern field theory:

Goldstone's theorem and chiral symmetry breaking. Then we review the standard model and the dynamical alternatives, technicolor, extended techninicolor, and top-color.

1.1 The Goldstone Theorem

In a classical field theory [9] the action of a field $\phi^i(x)$, is defined as

$$I[\phi^i(x)] = \int d^4x\, \mathcal{L}(\phi^i(x), \partial_\mu \phi^i(x)) \tag{1.1}$$

The fields that extremize the action, obey the equation of motion

$$\frac{\partial \mathcal{L}}{\partial \phi^i} = \partial_\mu \frac{\partial \mathcal{L}}{\partial(\partial_\mu \phi^i)} = \partial_\mu \Pi^{\mu i}, \tag{1.2}$$

where in the last step the canonical conjugate momentum $\Pi^{\mu i}$ has been introduced. A continuous transformation $\alpha : \phi^i(x) \longmapsto \phi^i(x, \alpha)$, where $\phi^i(x, 0) \equiv \phi^i(x)$ is called a *symmetry*, if the variation of the Lagrangian can be written as a four divergence of an arbitrary function $F(x)$:

$$\delta\mathcal{L} = \partial^\mu F_\mu, \qquad \text{where} \qquad \delta f \equiv \left.\frac{df}{d\alpha}\right|_{\alpha=0}. \tag{1.3}$$

It can be straightforwardly shown that, if the above holds, the action is invariant under the (infinitesimal) transformation α.

According to Noether's Theorem, the four-divergence of the current

$$j^\mu \equiv \Pi^\mu_i \delta\phi^i - F^\mu \tag{1.4}$$

vanishes, which yields the conserved charge $Q \equiv \int d^3x\, j^0$.

In a quantum field theory, following the approach through canonical quantization, ϕ^i

and $\Pi_i \equiv \Pi_i^0$ are promoted to operators which obey

$$\begin{aligned} [\phi^i(\vec{x},t), \Pi_j(\vec{y},t)] &= \imath\, \delta^i_j\, \delta^3(\vec{x}-\vec{y}), \\ [\phi^i(\vec{x},t), \phi^j(\vec{y},t)] &= 0 \\ \text{and} \quad [\Pi_i(\vec{x},t), \Pi_j(\vec{y},t)] &= 0 \end{aligned} \tag{1.5}$$

Starting with a symmetry group G, with elements $\exp(i\alpha_a T_a)$, where T_a are the *generators* of G, we can write an infinitesimal transformation of the field ϕ^i under G as

$$\phi^i \to \left(\delta^{ij} + \imath\alpha T_a^{ij}\right)\phi^j, \text{ so that } \delta_a\phi^i = \imath T_a^{ij}\phi^j. \tag{1.6}$$

In analogy to the case of a classical field theory one can define a current and its corresponding charge (whether conserved or not) as

$$j_a^\mu = \imath\, \Pi_i^\mu T_a^{ij}\phi^j \quad \Rightarrow \quad Q_a(t) = \imath \int d^3x\, \Pi_i(\vec{x},t) T_a^{ij}\phi^j(\vec{x},t)\,. \tag{1.7}$$

Using the equal time commutation relations from eq.(1.5), one can show that any local operator $\mathcal{O}(t)$ built out of the fields ϕ^i and the momenta Π_i obeys

$$[Q_a(t), \mathcal{O}(t)] = -\imath\, \delta_a \mathcal{O}(t)\,. \tag{1.8}$$

In particular, if the Hamiltonian of the theory commutes with the charge associated with the generator of the transformation, Q_a is conserved (time-independent) and thus *generates* a symmetry according to eq.(1.8).

In a quantum field theory, one postulates a state of lowest energy, the vacuum $|0\rangle$, as a normalizable eigenstate of the momentum operator with

$$P_\mu |0\rangle \;=\; 0\,. \tag{1.9}$$

A field theory with a symmetry, in the sense of the above definition, is said to experience a *spontaneous symmetry break down*[1] if and only if

$$\langle 0|\, \delta_a \psi(y)\, |0\rangle \;\neq\; 0 \tag{1.10}$$

for any field $\psi(y)$. This means that the vacuum expectation value of the field is not invariant under the symmetry transformation, even though the Hamiltonian is.

The *Goldstone Theorem* says that if a quantum field theory experiences a spontaneous symmetry break down, there is massless particle associated with each broken generator T_a in the spectrum.

Following [9] closely, we show that if for a quantum field theory with a conserved current j_a^μ every state but the vacuum has $p^\mu p_\mu \geq \epsilon$ for some $\epsilon > 0$, then $\langle 0|\delta\psi(y)|0\rangle = 0$ for all fields $\psi(y)$.

Proof:

$$\begin{aligned}
\langle 0|j_a^\mu(x)\psi(y)|0\rangle &= \sum_n \langle 0|j_a^\mu(x)|n\rangle\langle n|\psi(y)|0\rangle \\
&= \sum_n \langle 0|e^{\imath Px} j_a^\mu(0) e^{-\imath Px}|n\rangle\langle n|e^{\imath Py}\psi(0)e^{-\imath Py}|0\rangle \\
&= \sum_n \langle 0|j_a^\mu(0)|n\rangle\langle n|\psi(0)|0\rangle\, e^{\imath p_n(y-x)} \\
&= \int d^4k \sum_n \delta^4(k-p_n)\langle 0|j_a^\mu(0)|n\rangle\langle n|\psi(0)|0\rangle\, e^{\imath k(y-x)} \\
&\equiv \int d^4k\, k^\mu \rho_a(k^2)\, e^{\imath k(y-x)}
\end{aligned} \tag{1.11}$$

In the second last line, the sum over n does not give a contribution for $n = 0$, since $\langle 0|j_a^\mu(0)|0\rangle$ must be zero. By assumption, there is some $\epsilon > 0$ such that for $k^2 < \epsilon$, there is no other state with $p_n^2 < \epsilon$. This yields for $k^2 < \epsilon$: $\rho(k^2) = 0$.

[1]For a more intuitive introduction to spontaneous symmetry breaking in quantum field theories see for example [18].

Since the four divergence of j_a^μ vanishes, we can see from the last line $k^2\rho(k^2) = 0$, which yields $\rho(k^2)$ for $k^2 > 0$. Thus

$$\langle 0|j_a^\mu(x)\psi(y)|0\rangle = 0 \quad \text{(It analogously follows that } \langle 0|\psi(y)\, j_a^\mu(x)|0\rangle = 0) \tag{1.12}$$

This yields

$$\int d^3x\, \langle 0|[j_a^\mu(x), \psi(y)]|0\rangle = \langle 0|\delta_a\psi(y)|0\rangle = 0\,. \qquad \text{qed} \tag{1.13}$$

Inverting the statement of the proof tells us that if we have a spontaneous break down of a symmetry $\langle 0|\, \delta_a\, \pi_a(p)\, |0\rangle \neq 0$, there has to be a massless state in the spectrum. This state is called Goldstone boson and will be denoted as π_a. It has to couple to the conserved current, since if it did not, the above steps of the proof of the Goldstone theorem would yield eq.(1.13) in contradiction to the assumption of a symmetry break down. From the Lorenz structure of the current and the fact that its four divergence vanishes, we obtain

$$\langle 0|j_a^\mu(x)\pi_b(p)|0\rangle = \imath f_\pi p^\mu\, \delta_{ab}\, e^{\imath px}, \tag{1.14}$$

where the so-called *pion decay constant* f_π has been introduced as the strength of the coupling of the Goldstone boson to the conserved current.

1.2 Chiral Symmetry Breaking in massless QCD

In massless quantum chromodynamics[2] with the two quark-flavors u and d, if one neglects the electroweak interactions, the Lagrangian reads [9]

$$\mathcal{L} = \bar{q}_c \imath\gamma^\mu D_\mu^{cc'} q_{c'} - \frac{1}{2}\mathrm{tr}[F^{\mu\nu}F_{\mu\nu}], \tag{1.15}$$

[2]The typical energy scale of phenomena determined by QCD, Λ_{QCD} is of order of a few hundred MeV. It is therefore a reasonable approximation to assume m_u and m_d to be zero.

where $q = (u, d)$ and $D_\mu^{cc'}$ denotes the $SU(3)$-color gauge-covariant derivative

$$D_\mu^{cc'} = \partial_\mu \delta^{cc'} + \imath g_3 \, A_\mu^a \left(\frac{\lambda^a}{2}\right)^{cc'} . \tag{1.16}$$

In terms of the matrix valued fields $A_\mu \equiv A_\mu^a \frac{\lambda^a}{2}$, the field strength tensor reads

$$F_{\mu\nu} \;=\; \partial_\mu A_\nu \;-\; \partial_\mu A_\nu \;+\; \imath g_3 [A_\mu, A_\nu]. \tag{1.17}$$

The Lagrangian from eq.(1.15) is invariant under *local* $SU(3)$ transformations by construction[3]. Additionally, there is a global symmetry of the theory. In order to demonstrate this, we introduce the *chiral* projectors $P_{R/L} = \frac{1}{2}(1 \pm \gamma_5)$ which satisfy $P_R + P_L = 1$ and $P_R \, P_L = 0$. Defining $q_{L/R} = (u_{L/R}, d_{L/R}) \equiv P_{L/R}(u, d)$ and using $\{\gamma_5, \gamma_\mu\} = 0$, we can rewrite eq.(1.15) as

$$\mathcal{L} = \bar{q}_L \imath \not{\partial} q_L + \bar{q}_R \imath \not{\partial} q_R - \mathcal{L}_{gauge}. \tag{1.18}$$

This Lagrangian is manifestly invariant under *global* unitary transformations of the fermion fields $\mathcal{U}_L \times \mathcal{U}_R \;\in\; U(2)_L \times U(2)_R$ independently:

$$q_L \to \mathcal{U}_L q_L, \qquad q_R \to \mathcal{U}_R q_R \,. \tag{1.19}$$

It is generally believed that QCD dynamics induce a non-zero vacuum expectation value for the operator $\bar{q}q = \bar{q}_L q_L + \bar{q}_R q_R$. Since the formation of this *condensate* is assumed to occur because the non-Abelian color interactions become strong at Λ_{QCD}, there is no mathematical proof, because at this point the perturbative calculational tools break down. But assuming that this is what happens leads to impressive predictions, as we shall see in the following.

From

$$\langle \bar{q}_L q_L + \bar{q}_R q_R \rangle \neq 0, \tag{1.20}$$

[3]For a detailed discussion of gauge theories, see e.g. chapter 15 in [15].

we see that the vacuum expectation value is no longer invariant under separate $U(2)_L$ and $U(2)_R$ transformations. However, it remains invariant under $U(2)_V$ ("vector"-) transformations:

$$\mathcal{U}_V = \mathcal{U}_L = \mathcal{U}_R = \exp[\imath\theta_V] \exp[\imath\alpha_V^a \frac{\tau^a}{2}], \tag{1.21}$$

where $\alpha = 1, 2, 3$ and τ^a are the usual Pauli-matrices.

We write the original symmetry group as a direct product according to

$$U(2)_L \times U(2)_R \;=\; U(1)_V \times U(1)_A \times SU(2)_V \times \text{"}SU(2)_A\text{"}, \tag{1.22}$$

where the subscript A stands for axial vector transformations, which are generated by

$$\begin{aligned} \exp[\imath\theta_A\gamma_5] &= \exp[\imath\theta_A]P_R + \exp[-\imath\theta_A]P_L \qquad \text{for } U(1)_A \\ \exp[\imath\theta_A\frac{\tau^a}{2}\gamma_5] &= \exp[\imath\alpha_A^a\frac{\tau^a}{2}]P_R + \exp[-\imath\alpha_A^a\frac{\tau^a}{2}]P_L \qquad \text{for "}SU(2)_A\text{"}. \end{aligned} \tag{1.23}$$

Note that $SU(2)_A$ does actually not form a proper subgroup, because the algebra of its generators $\frac{\tau^a}{2}\gamma_5$ does not close. But since we only need the infinitesimal transformations, regardless of whether they form a group or not, this is not important.

Even though eq.(1.22) is the symmetry group of the Lagrangian from eq.(1.18), quantum effects actually spoil the invariance of the theory under $U(1)_A$ right away.[4] So only "$SU(2)_A$" is broken by the appearance of the non-trivial vacuum expectation value in eq.(1.20). Therefore we expect three massless Goldstone bosons in the spectrum which couple to the currents associated with the spontaneously broken generators of the symmetry "$SU(2)_A$"

$$j_5^{\mu a} = \Pi^\mu \delta^a q = \bar{q}\gamma^\mu\gamma_5\frac{\tau^a}{2}q \tag{1.24}$$

[4]For details see chapter 19 in [15].

according to

$$\langle 0|j_5^{\mu a}(0)|\pi^b(q)\rangle = \imath f_\pi \, q^\mu \, \delta^{ab} \,. \tag{1.25}$$

Since the current $j_5^{\mu a}$ transforms as axial-vector under parity transformations and on the right-hand side of the equation stands a Lorenz vector, we can conclude that the Goldstone bosons have to transform as pseudo-scalars under parity.

The behavior of the Goldstone bosons under the (unbroken) symmetry transformations can be determined by looking at the commutator of the unbroken charges with $j_5^{\mu a}$. One obtains that they form a triplet under $SU(2)_V$ ("isospin") and have charge zero under $U(1)_V$ ("baryon number"). This isotriplet of Goldstone bosons is taken to be the triplet of the lightest experimentally observed hadrons, the pions whose masses are not exactly zero, albeit small compared to Λ_{QCD}. The pion decay constant is found to be $f_\pi \approx 93$ MeV.

In reality, the quarks have masses, which explicitly breaks the axial symmetries and if m_u and m_d are not degenerate, also breaks $SU(2)_V$. Since the masses and their difference are small, one assumes the symmetry group from eq.(1.22) to be an "approximate symmetry" of the Lagrangian in eq.(1.18). This leads to a pion mass proportional to its constituent masses (see [9]).

1.3 The Standard Model

The Glashow-Weinberg-Salam theory [18] of the weak interactions, which is generally referred to as the "standard model" starts from a Lagrangian that is gauge-invariant under the gauge group $SU(2)_L \times U(1)_Y$, where the subscript Y denotes the so-called hypercharge. For simplicity we shall sketch the model only for one family[5]

[5]In reality there have been observed three generations of fermions. The other two generations can be seen, within the standard model, as replicates of the first generations with heavier masses.

of fermions e, ν, u, d,. The left handed fermions ($f_L \equiv P_L f$, where P_L denotes the chiral projector as defined in the previous section) transform as doublets under $SU(2)_L$, $E_L = (\nu_L, e_L)_{Y=-1/2}$ for leptons and $Q_L = (u_L, d_L)_{Y=1/6}$. The right handed fermions are singlets with respect to $SU(2)_L$ and their hypercharge assignments are chosen to be equal to their electric charge, for reasons, that will become obvious later.

The Lagrangian describing the interactions of fermions with the gauge fields and among the gauge bosons themselves reads

$$\mathcal{L}_{fermions} = \sum_f \imath \gamma^\mu \bar{f} D_\mu f - \frac{1}{4} F^{\mu\nu} F_{\mu\nu} - \frac{1}{4} G^{a\mu\nu} G^a_{\mu\nu}, \tag{1.26}$$

with

$$D_\mu = \partial_\mu + \imath g' B_\mu Y + \imath g \tau^a W^a_\mu . \tag{1.27}$$

The sum runs over all left- and right-handed fermions.[6] B^μ denotes the gauge field associated with $U(1)_Y$ and W^a_μ represents the triplet of the $SU(2)_L$ gauge fields. The $\tau^a \equiv \sigma^a/2$, where σ^a denote the Pauli matrices, are the generators of $SU(2)_L$. The last two terms in eq.(1.26) represent the kinetic Lagrangian for the gauge bosons.

A key ingredient to the standard model is a complex doublet scalar field, $\phi \equiv (\phi^+, \phi^0)_{Y=1/2}$. As we shall see in the following it drives the symmetry breaking creating the masses of the heavy gauge bosons. It is also responsible for the generation of fermion masses in this model. Its dynamics are described by

$$\mathcal{L}_{scalar} = (D_\mu \phi)^\dagger (D^\mu \phi) - V(\phi^\dagger \phi), \tag{1.28}$$

with the covariant derivative from eq.(1.27) and a potential of the form

$$V(\phi^\dagger \phi) \equiv \mu^2 \left(\phi^\dagger \phi\right) + |\lambda| \left(\phi^\dagger \phi\right)^2 . \tag{1.29}$$

[6]Note, that since the right handed fermions are singlets under $SU(2)_L$ they are eigenvectors of the $SU(2)_L$ generators τ^a corresponding to the eigenvalue zero.

Additionally, we are free to add an interaction term via Yukawa couplings of the scalar doublet to the fermions

$$\mathcal{L}_{Yukawa} = -G_e \bar{E}_L \phi e_R - G_u \bar{Q}_L \phi u_R - G_d \epsilon^{ab} \bar{Q}_{La} \phi_b^\dagger d_R + h.c. \tag{1.30}$$

This term is gauge-invariant under $SU(2)_L \times U(1)_Y$. The mass of the neutrinos in this simple version of the model is assumed to be zero, which is equivalent to excluding right- handed neutrinos from the beginning.

If we let the parameter μ in eq.(1.29) be negative, the potential has a continuous set of non-trivial degenerate minima, implicitly given by $|\phi_{min}|^2 = (-\mu^2/2|\lambda|) \equiv v^2/2$. We choose the vacuum expectation value of the scalar field to be

$$\langle \phi \rangle \equiv \langle 0|\phi|0\rangle = \begin{pmatrix} 0 \\ \frac{v}{\sqrt{2}} \end{pmatrix}, \tag{1.31}$$

which obviously breaks the generators of the gauge groups $SU(2)_L \times U(1)_Y$, except from the linear combination

$$(\tau_3 + Y) \langle \phi \rangle \equiv Q \langle \phi \rangle, \tag{1.32}$$

which is identified with the electric charge Q. Unlike in QCD where a global symmetry broke down, no Goldstone bosons appear in the spectrum, but they become the longitudinal polarizations of the formerly massless gauge bosons associated with the broken generators. One can see this by expanding the scalar field around its vacuum expectation value:

$$\phi = \exp\left(i \frac{\alpha^a(x)\tau^a}{2v}\right) \begin{pmatrix} 0 \\ \frac{(h(x)+v)}{\sqrt{2}} \end{pmatrix}, \tag{1.33}$$

which is gauge-equivalent to

$$\phi \rightarrow \phi' = \begin{pmatrix} 0 \\ \frac{(h(x)+v)}{\sqrt{2}} \end{pmatrix}. \tag{1.34}$$

Inserting this into eq.(1.28), we find

$$\mathcal{L}_{scalar} = \frac{1}{2}\left(\partial_\mu h\right)^2 - \mu^2 h^2 + \frac{1}{4}\frac{v^2}{2}\left(g^2\left(W_\mu^1\right)^2 + g^2\left(W_\mu^2\right)^2 + \left(-gW_\mu^3 + g'B_\mu\right)^2\right)$$
$$+ \text{“interaction terms”} \,. \tag{1.35}$$

The term proportional to v^2 has the form of a mass term for three massive vector bosons. Defining the *weak mixing angle* via

$$\cos\theta \equiv \frac{g}{\sqrt{g^2 + g'^2}} \tag{1.36}$$

allows us to denote them as follows:[7]

$$W_\mu^\pm = \frac{1}{\sqrt{2}}\left(W_\mu^1 \mp \imath W_\mu^2\right) \qquad \text{with mass} \quad m_W = g\frac{v}{2}\,; \tag{1.37}$$

$$Z_\mu^0 = \left(\cos\theta W_\mu^3 - \sin\theta B_\mu\right) \qquad \text{with mass} \quad m_Z = \frac{v}{2}\sqrt{g^2 + g'^2}\,. \tag{1.38}$$

The fourth vector field, orthogonal to Z_μ^0, remains massless and is identified with the photon

$$A_\mu = \left(\sin\theta W_\mu^3 + \cos\theta B_\mu\right). \tag{1.39}$$

In order to obtain the couplings of the mass eigenstates it is useful to replace the canonical gauge fields in the covariant derivative from eq.(1.27) by the appropriate linear combinations of the mass eigenstates:

$$D_\mu = \partial_\mu - \imath\frac{g}{\sqrt{2}}\left(W_\mu^+\tau^+ + W_\mu^-\tau^-\right) - \imath Z_\mu\left(g\cos\theta\,\tau^3 - g'\sin\theta\, Y\right)$$
$$-\imath\frac{g'g}{\sqrt{g^2 + g'^2}}A_\mu\left(\tau^3 + Y\right), \tag{1.40}$$

where $\tau^\pm = 1/2(\sigma^1 \pm \imath\sigma^2)$. In order to complete the association of the residual $U(1)$ gauge symmetry with electrodynamics, we define

$$e = \frac{g'g}{\sqrt{g^2 + g'^2}}. \tag{1.41}$$

[7]Comparison to low-energy measurements where the weak interactions appear as effective four fermion interactions, allows us to relate the vacuum expectation value of the scalar condensate to the *Fermi-constant* according to $v = (\sqrt{2}G_F)^{(-1/2)} \approx 264$ GeV.

The first two terms in eq.(1.35) describe the physical "Higgs"-particle with mass $m_H = -\sqrt{2}\mu > 0$.

The Yukawa-coupling of the fermions to the scalar field in eq.(1.30) gives rise to fermion masses and fermion-Higgs interactions:

$$\mathcal{L}_{Yukawa} = -\sum_f G_f \frac{v+h}{\sqrt{2}} \left(\bar{f}_L f_R + \bar{f}_R f_L\right) \quad \Rightarrow \quad m_f = G_f \frac{v}{\sqrt{2}} \,. \tag{1.42}$$

One can picture the fermions acquiring mass as an effect of their motion through an "ether" consisting of the condensates of the scalar field:

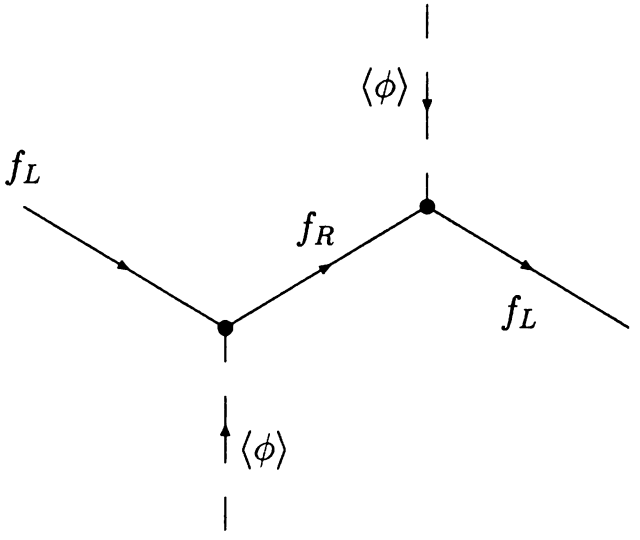

1.4 Technicolor

The standard model as described in the previous section has proven to be extremely successful describing what has been measured in experiments so far. Nevertheless, the existence of a fundamental scalar field gives rise to conclusions of unsatisfactory character:

- The bare existence of a fundamental scalar field has no observed analogy in

experiments so far.

- Loop corrections lead to a quadratically divergent mass correction to the tree-level mass of the physical Higgs-field $h(x)$ as derived in the previous section. If one wants the theory to be valid up to high energy scales, this leads to a severe fine-tuning problem [19].

- Beyond the requirement of gauge invariance, there are no further constraints on the self-coupling of the Higgs field or on its Yukawa-couplings to the fermions. Hence, we are left with a large number of free parameters.

Technicolor addresses mainly the first two statements. In this theory there is no fundamental scalar particle. The electroweak symmetry breaking is achieved by employing an analogy to QCD [10] as described in section 1.2.
In a massless two-flavor version of QCD the Lagrangian is invariant under *global*

$$SU(2)_L \times SU(2)_R \times U(1)_V, \tag{1.43}$$

transformations. Further we assume the existence of a *gauged* subgroup of eq.(1.43)

$$SU(2)_L \times U(1)_Y\,. \tag{1.44}$$

So we have four massless gauge fields of the unbroken standard model $W_\mu^\pm$, W_μ^0, B_μ, in addition to the discussion in section 1.2. At Λ_{QCD} the chiral symmetry breaks down to $SU(2)_V \times U(1)_V$, which would make three massless Goldstone bosons appear in the spectrum, if not for the presence of the gauge fields in this case. The interaction of the massless gauge bosons with the pions shifts the propagator of the $W_\mu^\pm$ according to

$$\Delta^{\mu\nu} = \frac{g^{\mu\nu} - q^\mu q^\nu/q^2}{q^2} \;\rightarrow\; \frac{g^{\mu\nu} - q^\mu q^\nu/q^2}{q^2(1+\Pi(q^2))} \tag{1.45}$$

where $\Pi(q^2)$ denotes the vacuum polarization. The process is schematically shown in the diagram below.

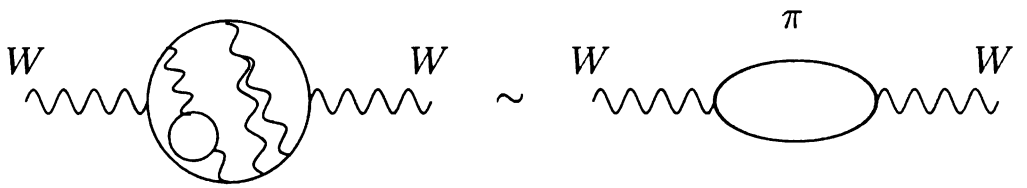

Figure 1.1. Coupling of the $W^{\pm}$ bosons to the pions.

Since the pion is massless, its propagator has a pole at $q^2 \to 0$. The current $j^5_{\pm 5}$ couples to $\pi^{\mp}$ with strength f_π, which yields a contribution to $\Pi(q^2)$ according to

$$\lim_{q^2 \to 0} \Pi(q^2) \to \frac{g^2 f_\pi^2}{4q^2}. \tag{1.46}$$

This shifts the pole in the propagator in eq.(1.45) to $\frac{1}{4}g^2 f_\pi^2$, so the $W^{\pm}_\mu$ gauge field has acquired a mass of $m_W = \frac{1}{2} g f_\pi$. An analogous, albeit more complicated, calculation yields a massless photon- and a Z^0_μ-analog with the mass from eq.(1.38), with f_π instead of v.

So the chiral symmetry breaking in QCD breaks the standard model gauge group $SU(2)_L \times U(1)_Y$ down to $U(1)_Q$ and the pions become the longitudinal components of the electroweak gauge bosons. Unfortunately, the masses of the gauge bosons are too light (by a factor of ≈ 2600).

The idea of Technicolor is now to introduce a new type of fermion, the *technifermions*, which have a new strong gauge interaction, but where the chiral symmetry breaking occurs at a higher scale[8] $\Lambda_{TC} \gg \Lambda_{QCD}$, such that the *technipion decay constant* F_π can be numerically equal to the vacuum expectation value of the standard model scalar field v. From the above calculation we see that this yields the correct masses

[8]This suggests that the technifermions have an $SU(N)_{TC}$ gauge interaction whose coupling becomes strong at a higher scale Λ_{TC}.

for the weak bosons.

Various models involving different sets of technifermions have been studied (see e.g.[10],[12]). The simplest model, providing the correct symmetry breaking pattern, consists of only one $SU(2)_L$ doublet of technifermions

$$T_L = \begin{pmatrix} A_L \\ B_L \end{pmatrix}_{Y=0}, \quad (A_R)_{Y=1/2}, \quad (B_R)_{Y=-1/2}. \tag{1.47}$$

The technifermions are color-singlets, but transform as a non-trivial representation of technicolor $SU(N)_{TC}$. In this model there are only three exact Goldstone bosons, the technipions.[9] So the techni-hadronic spectrum consists of the analogs to the hadrons in massless two-flavor QCD. Their masses are estimated by scaling up the masses of their QCD-analogs by $\Lambda_{TC}/\Lambda_{QCD}$ (see again the references given above). The existence of the technihadrons also plays an important role in the unitarization of W-scattering.

More realistic scenarios provide, besides the three technipions as exact Goldstone-bosons, a rich spectrum of "Pseudo-Goldstone-Bosons" which acquire mass due to their non-trivial transformation behavior under the standard model gauge groups [10].

1.5 Extended Technicolor

Although technicolor models can explain the mechanism of electroweak symmetry breaking, they do not provide a complete theory that could replace the standard model, since they cannot give an explanation for the generation of fermion masses.

[9]The "eaten" and the physical pions are actually linear combinations of the technipions and the QCD-pions, but since the decay constants appear as weights in the linear combination and $F_\pi \gg f_\pi$, the physical pions consist in good approximation only of the QCD-pions and the eaten pions are mainly technipions.

Extended technicolor (ETC) ([12] and references therein), as the name indicates, is a model which preserves the technicolor-scheme for the electroweak symmetry breaking and adds a mechanism creating the masses of the fermions.

The idea is to embed the technicolor gauge group $SU(N)_{TC}$ and possibly parts of the full gauge group

$$SU(N)_{TC} \times SU(3)_c \times SU(2)_L \times U(1)_Y \tag{1.48}$$

into a larger gauge group $\mathcal{G}_{ETC}$. At a high scale $\Lambda_{ETC} \gg \Lambda_{TC}$ the ETC gauge group $\mathcal{G}$ breaks down, giving masses to the ETC gauge bosons which mediate interactions among technifermions and ordinary fermions. This can be seen in the following example [10]:

> Suppose having a technicolor gauge group $SU(N)_{TC}$ and some technifermions in its fundamental representation (N-dim). Now embed the technifermions in $SU(N+1)_{ETC}$, which somehow breaks down to $SU(N)_{TC}$. This leaves us with an N-tuple of technifermions and a singlet under technicolor, an ordinary fermion. The broken generators are exactly those $2N+1$ generators of $SU(N+1)_{ETC}$ which had "mixed" the N technifermions with the additional component of the $N+1$-dim fundamental representation of $SU(N+1)_{ETC}$.

The fermion masses are assumed to be generated by the following mechanism, which is sketched in Figure 1.2:

The interactions of massive ETC gauge bosons ($m_{ETC} \approx \Lambda_{ETC}$) with the fermions can be, at energies well below Λ_{ETC}, described as an effective four fermion interaction

$$\mathcal{L} \propto \left(\frac{g_{ETC}}{\Lambda_{ETC}}\right)^2 (\bar{F}\gamma^\mu T^a f)(\bar{f}\gamma_\mu T^a F) \tag{1.49}$$

where F denotes the technifermions, f the ordinary fermions and T^a are the broken generators of $\mathcal{G}_{ETC}$. A Fierz-rearrangement of this Lagrangian contains a term of the form

$$-\left(\frac{g_{ETC}}{\Lambda_{ETC}}\right)^2 [(\bar{F}_L F_R)(\bar{f}_L f_R) + h.c. + \ldots] \tag{1.50}$$

such that at energies below $\Lambda_{TC} \approx 0.5 - 1.0$ TeV, where the technifermions condense $\langle \bar{F}F \rangle \neq 0$, this takes the form of a mass term with $m_f \approx g^2_{ETC} \frac{\langle \bar{F}F \rangle_{vac}}{\Lambda^2_{ETC}}$.

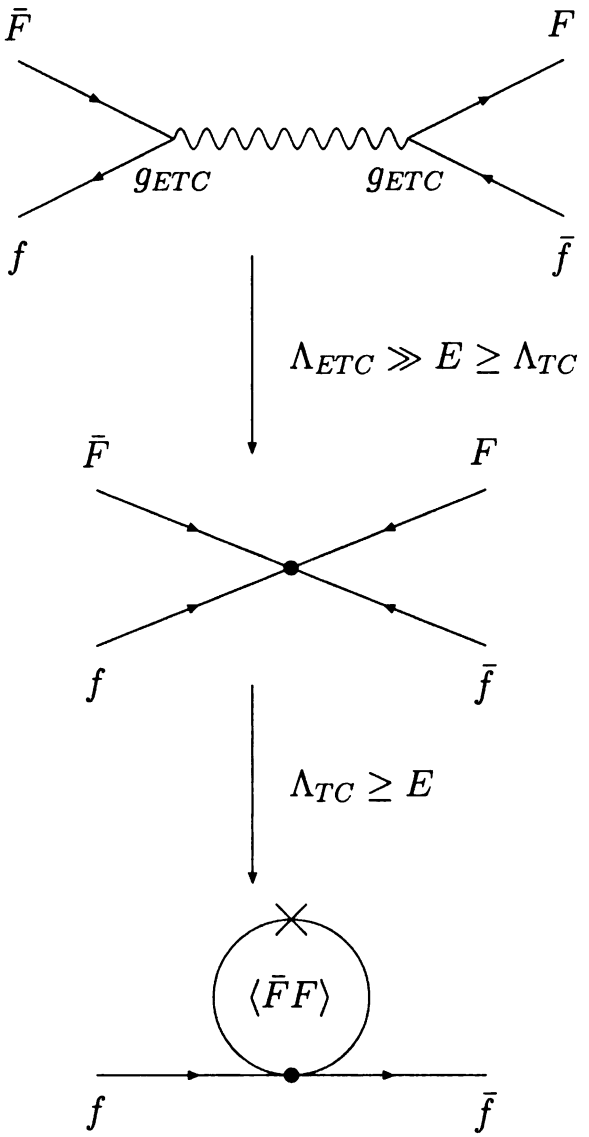

Figure 1.2. The generation of the fermion masses in extended technicolor. In the last step, the technicolor interaction becomes strong and closes the external technifermion lines to a loop.

The extended technicolor gauge bosons cause flavor changing neutral currents, which forces the scale Λ_{ETC} to be very large, in order not to disagree with the experimental results from for e.g. the measurement of the kaon mass-splitting. At this very high scale, the coupling constant of the ETC-group is very small. This makes it difficult

to generate fermion masses of the appropriate size.[10] A possible solution may be a so-called "walking" of the technicolor coupling constant [13] up to Λ_{ETC}. It is generally believed that this can explain masses up to the bottom quark mass.

1.6 Topcolor

The extremely high mass of the top-quark suggests that there are extra dynamics associated with the top-sector that single out the top-quark. The idea of topcolor [11] is to introduce a strong interaction, that makes the top-quark form a condensate and thus dynamically creates the top-mass via the coupling of the top-quark to its condensate, in analogy to the mass generation for the light fermions in extended technicolor models.

Various ansätze have been discussed in the past [12]. The subject of our work is a topcolor model with a flavor universal hypercharge sector and how its parameter space is constrained by existing data from experiments.

[10] The ratios of the different fermion masses can be adjusted, but the problem is to create the right absolute size. Even the charm quark mass can barely be realized.

Chapter 2

Topcolor with a Flavor-Universal Hypercharge Sector

We start from the gauge group

$$SU(3)_1 \times SU(3)_2 \times SU(2) \times U(1)_1 \times U(1)_2, \tag{2.1}$$

where the corresponding couplings are chosen such that $g_{3(1)} > g_{3(2)}$. Quarks and leptons transform only under the stronger $U(1)$ group and in the color sector the third generation of quarks transforms under the stronger $SU(3)$, whereas the light quarks transform under the weaker $SU(3)$ group.

gen	$SU(3)_1$	$SU(3)_2$	$SU(2)$	$U(1)_1$	$U(1)_2$
I,II	1	"SM"	"SM"	"SM"	0
III	"SM"	1	"SM"	"SM"	0
Φ_Λ	3	$\bar{3}$	1	$\frac{p}{2\sqrt{6}}$	$-\frac{p}{2\sqrt{6}}$
ϕ_{TC}	1	1	2	0	$\frac{1}{2}$
φ_t	1	1	2	$-\frac{1}{2}$	0

Table 2.1. The transformation behavior of the fermion generations and the composite scalars under the gauge group from eq.(2.1). "SM" means that the fermions transform under the respective group as they would under the corresponding standard model gauge group.

At the scale Λ

$$\Lambda_{ETC} > \Lambda > \Lambda_{weak}, \tag{2.2}$$

a condensate $\langle \Phi_\Lambda \rangle = F_\Lambda \, \delta_{\alpha\beta}$, that transforms under the initial gauge group in eq.(2.1) according to Table 2.1 forms, which breaks the color sector and the hypercharge groups into their diagonal subgroups[1]:

$$SU(3)_1 \times SU(3)_2 \to SU(3)_C, \quad U(1)_1 \times U(1)_2 \to U(1)_Y \tag{2.3}$$

This symmetry breaking also triggers the condensation of top quarks $\langle \varphi_t \rangle$ at a much lower scale. The discussion of this mechanism shall be postponed to section 2.3.

The remaining standard model electroweak gauge group is then broken by the technifermion and the top condensate

$$\langle \phi_{TC} \rangle = \begin{pmatrix} 0 \\ \frac{F_{TC}}{\sqrt{2}} \end{pmatrix}, \qquad \langle \varphi_t \rangle = \begin{pmatrix} 0 \\ \frac{f_t}{\sqrt{2}} \end{pmatrix} \tag{2.4}$$

according to

$$SU(3)_c \times SU(2)_L \times U(1)_Y \to U(1)_Q. \tag{2.5}$$

2.1 Symmetry Breaking at the Scale Λ

The relevant part of the Lagrangian (i.e. omitting the $SU(2)$ gauge fields for this discussion) is given by

$$\mathcal{L} = \bar{\Psi} \imath \not{D} \Psi + \mathrm{tr} \left(D_\mu \Phi_\Lambda \right)^\dagger D^\mu \Phi_\Lambda + \mathcal{L}_{Gauge}, \tag{2.6}$$

with

$$D_\mu = \partial_\mu + \imath g_{3(1)} A^a_{1\mu} T^a_1 + \imath g_{3(2)} A^a_{2\mu} T^a_2 + \imath g_{1(1)} B_{1\mu} Y_1 + \imath g_{1(2)} B_{2\mu} Y_2 \tag{2.7}$$

[1]Within this thesis we will not specify the nature of this particle any further. We will just investigate the implications of this model for low-energy physics.

where $T^a = \frac{\lambda^a}{2}$ are the generators of $SU(3)$. A^{1a}_μ and A^{2a}_μ are the $SU(3)$ gauge fields and B^1_μ and B^2_μ, the fields associated with the respective $U(1)$ gauge groups. $\mathcal{L}_{Gauge}$ denotes the gauge kinetic terms for all four gauge fields.

According to the Goldstone theorem (see section 1.1), there appears one massless particle associated with each generator of a broken *global* symmetry. In this case, a *local* symmetry is broken, which triggers the Higgs-mechanism and makes the Goldstone bosons become the longitudinal components of the gauge fields, belonging to the broken generators. In other words, these gauge bosons acquire mass as the massless Goldstone bosons vanish from the spectrum.

To demonstrate this, we look at the zeroth order term of the expansion of the field Φ_Λ around its vacuum expectation value $\langle\Phi_\Lambda\rangle$. The covariant derivative from eq.(2.7) acting on $\langle\Phi_\Lambda\rangle$ gives[2]

$$\begin{aligned} D_\mu \langle\Phi_\Lambda\rangle = \partial_\mu \langle\Phi_\Lambda\rangle &+ \imath g_{3(1)} A^a_{1\mu} \left(\tfrac{\lambda^a}{2}\right) \langle\Phi_\Lambda\rangle - \imath g_{3(2)} A^a_{2\mu} \langle\Phi_\Lambda\rangle \left(\tfrac{\lambda^a}{2}\right) \\ &+ \imath g_{1(1)} B_{1\mu} Y_1 \langle\Phi_\Lambda\rangle + \imath g_{1(2)} B_{2\mu} Y_2 \langle\Phi_\Lambda\rangle \\ = \quad &\imath\Lambda \left(\tfrac{\lambda^a}{2}\right) \left(g_{3(1)} A^a_{1\mu} - g_{3(2)} A^a_{2\mu}\right) \\ &+ \imath\Lambda \tfrac{p}{2\sqrt{6}} \left(g_{1(1)} B_{1\mu} - g_{1(2)} B_{2\mu}\right) \end{aligned} \tag{2.8}$$

[2]The minus sign in the first line of eq.(2.8) accounts for the condensate transforming, according to Table 2.1, under the *conjugate* representation of $SU(3)_2$.

Inserting this in the kinetic term of Φ_Λ in eq.(2.6) yields

$$
\begin{aligned}
&\mathrm{tr}[(D_\mu \langle\Phi\rangle\ )^\dagger (D^\mu \langle\Phi\rangle\ )] \\
&= \Lambda^2 \Big[\underbrace{\mathrm{tr}\left[\left(\frac{\lambda^a}{2}\right)\left(\frac{\lambda^b}{2}\right)\right]}_{=\frac{1}{2}\delta^{ab}} \left(-\imath g_{3(1)} A^a_{1\mu} + \imath g_{3(2)} A^a_{2\mu}\right)\left(\imath g_{3(1)} A^{b\mu}_1 - \imath g_{3(2)} A^{b\mu}_2\right) \\
&\qquad + \underbrace{\mathrm{tr}[1]}_{=3} \frac{p^2}{24}\left(-\imath g_{1(1)} B_{1\mu} + \imath g_{1(2)} B_{2\mu}\right)\left(\imath g_{1(1)} B^\mu_1 - \imath g_{1(2)} B^\mu_2\right)\Big] \\
&= \frac{\Lambda^2}{2} \begin{pmatrix} A^a_{1\mu} \\ A^a_{2\mu} \\ B_{1\mu} \\ B_{2\mu} \end{pmatrix}^T \begin{pmatrix} g^2_{3(1)} & -g_{3(1)}g_{3(2)} & 0 & 0 \\ -g_{3(1)}g_{3(2)} & g^2_{3(2)} & 0 & 0 \\ 0 & 0 & \left(\frac{p}{2}\right)^2 g^2_{1(1)} & \left(\frac{p}{2}\right)^2 g_{1(1)}g_{1(2)} \\ 0 & 0 & -\left(\frac{p}{2}\right)^2 g_{1(1)}g_{1(2)} & \left(\frac{p}{2}\right)^2 g^2_{1(2)} \end{pmatrix} \begin{pmatrix} A^{a\mu}_1 \\ A^{a\mu}_2 \\ B^\mu_1 \\ B^\mu_2 \end{pmatrix}
\end{aligned}
\tag{2.9}
$$

The upper block of the matrix appearing in the last step can be diagonalized, by rotating to the basis of the mass eigenstates:

$$G^{a\mu} = \frac{g_{3(2)} A^{a\mu}_1 + g_{3(1)} A^{a\mu}_2}{\sqrt{g^2_{3(1)} + g^2_{3(2)}}}, \tag{2.10}$$

$$C^{a\mu} = \frac{g_{3(1)} A^{a\mu}_1 - g_{3(2)} A^{a\mu}_2}{\sqrt{g^2_{3(1)} + g^2_{3(2)}}}, \tag{2.11}$$

where the first octet of fields belongs to the eigenvalue zero and is thus identified with the massless gluon and the second octet is the so called top gluon, with mass

$$M^2_C = \Lambda^2 \left(g^2_{3(1)} + g^2_{3(2)}\right). \tag{2.12}$$

An analogous diagonalization can be performed with the lower block of the matrix in eq.(2.9), yielding the massless B'_μ and the massive field Z'

$$B'^\mu = \frac{g_{1(2)} B^\mu_1 + g_{1(1)} B^\mu_2}{\sqrt{g^2_{1(1)} + g^2_{1(2)}}}, \tag{2.13}$$

$$Z'^\mu = \frac{g_{1(1)} B^\mu_1 - g_{1(2)} B^\mu_2}{\sqrt{g^2_{1(1)} + g^2_{1(2)}}}. \tag{2.14}$$

The mass of the Z' boson is then given by

$$M_{Z'}^2 = \frac{p^2}{4}\Lambda^2 \left(g_{1(1)}^2 + g_{1(2)}^2\right) \tag{2.15}$$

The gauge covariant derivative from eq.(2.7) can then be expressed in terms of the mass eigenstates:

$$\begin{aligned} D_\mu = \partial_\mu &+ \imath g_{3(1)} \left(\cos\omega\, C_\mu^a + \sin\omega\, G_\mu^a\right) T_1^a + \imath g_{3(2)} \left(-\sin\omega\, C_\mu^a + \cos\omega\, G_\mu^a\right) T_2^a \\ &+ \imath g_{1(1)} \left(\cos\phi\, Z'_\mu + \sin\phi\, B'_\mu\right) Y_1 + \imath g_{1(2)} \left(-\sin\phi\, Z'_\mu + \cos\phi\, B'_\mu\right) Y_2, \end{aligned} \tag{2.16}$$

where the notation

$$\cos\omega = \frac{g_{3(1)}}{\sqrt{g_{3(1)}^2 + g_{3(2)}^2}}, \qquad \sin\omega = \frac{g_{3(2)}}{\sqrt{g_{3(1)}^2 + g_{3(2)}^2}} \tag{2.17}$$

$$\cos\phi = \frac{g_{1(1)}}{\sqrt{g_{1(1)}^2 + g_{1(2)}^2}}, \qquad \sin\phi = \frac{g_{1(2)}}{\sqrt{g_{1(1)}^2 + g_{1(2)}^2}} \tag{2.18}$$

has been used.

The interactions of fermions with the massive vector bosons, arising from the fermionic kinetic term in the Lagrangian in eq.(2.6), then have the form

$$\mathcal{L}_{int\,C} = \left[g_{3(1)} \cos\omega\, \bar{\psi}_{III}\, \gamma^\mu \left(\frac{\lambda^a}{2}\right) \psi_{III} - g_{3(2)} \sin\omega\, \bar{\psi}_{I,II}\, \gamma^\mu \left(\frac{\lambda^a}{2}\right) \psi_{I,II}\right] C_\mu^a, \tag{2.19}$$

$$\mathcal{L}_{int\,Z'} = g_{1(1)} \cos\phi\, \left(\bar{f}\gamma^\mu f\right) Y^f\, Z'_\mu, \tag{2.20}$$

where Ψ_i denotes the quark fields of the i-th generation and f any fermion field. This suggests that we define the coupling of the Z' to the fermions and the coupling of the top gluon to the third quark generation as

$$\kappa_1 \equiv \frac{g_{1(1)}^2}{\sqrt{g_{1(1)}^2 + g_{1(2)}^2}}, \qquad \kappa_3 \equiv \frac{g_{3(1)}^2}{\sqrt{g_{3(1)}^2 + g_{3(2)}^2}}, \tag{2.21}$$

respectively. The analogous expressions to eq.(2.19) and (2.20) describing the interactions of the massless vector bosons are given by

$$\mathcal{L}_{int\,G} = \left[g_{3(1)} \sin\omega\, \bar{\psi}_{III}\, \gamma^\mu \left(\frac{\lambda^a}{2}\right) \psi_{III} + g_{3(2)} \cos\omega\, \bar{\psi}_{I,II}\, \gamma^\mu \left(\frac{\lambda^a}{2}\right) \psi_{I,II} \right] G^a_\mu$$
$$= \frac{g_{3(1)} g_{3(2)}}{\sqrt{g^2_{3(1)} + g^2_{3(2)}}} \left[\bar{\Psi} \gamma^\mu \left(\frac{\lambda^a}{2}\right) \Psi \right] G^a_\mu, \tag{2.22}$$

$$\mathcal{L}_{int\,B'} = g_{1(1)} \sin\phi\, \left(\bar{f}\gamma^\mu f\right) Y^f\, B'_\mu = \frac{g_{1(1)} g_{1(2)}}{\sqrt{g^2_{1(1)} + g^2_{1(2)}}} \left(\bar{f}\gamma^\mu f\right) Y^f\, B'_\mu. \tag{2.23}$$

The respective couplings of the bosons associated with the unbroken gauge groups are defined as

$$g_3 \equiv \frac{g_{3(1)} g_{3(2)}}{\sqrt{g^2_{3(1)} + g^2_{3(2)}}} \quad \text{and} \quad \alpha_S \equiv \frac{g_3^2}{4\pi}$$
$$g' \equiv \frac{g_{1(1)} g_{1(2)}}{\sqrt{g^2_{1(1)} + g^2_{1(2)}}} \quad \text{and} \quad \alpha_Y \equiv \frac{g'^2}{4\pi} \tag{2.24}$$

Rewriting eqns.(2.19) and (2.20) in terms of κ_3, α_S and κ_1, α_Y yields

$$\mathcal{L}_{int\,C} = \sqrt{4\pi} \left[\sqrt{\kappa_3}\, \bar{\psi}_{III}\, \gamma^\mu \left(\frac{\lambda^a}{2}\right) \psi_{III} - \frac{\alpha_S}{\sqrt{\kappa_3}}\, \bar{\psi}_{I,II}\, \gamma^\mu \left(\frac{\lambda^a}{2}\right) \psi_{I,II} \right] C^a_\mu \tag{2.25}$$

$$\mathcal{L}_{int\,Z'} = \kappa_1\, \left(\bar{f}\gamma^\mu f\right) Y^f\, Z'_\mu \tag{2.26}$$

These Lagrangians give rise to processes as sketched below.

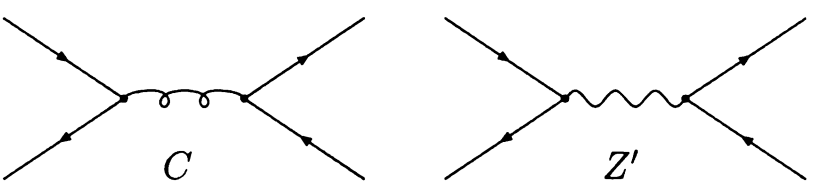

Figure 2.1. Interaction of fermions via Topgluon and Z'-boson exchange.

Since the gauge boson masses are presumably at least of order of a few TeV, one can, for processes with a momentum transfer well below this energy, integrate out the intermediate vector bosons. The effective four fermion interactions

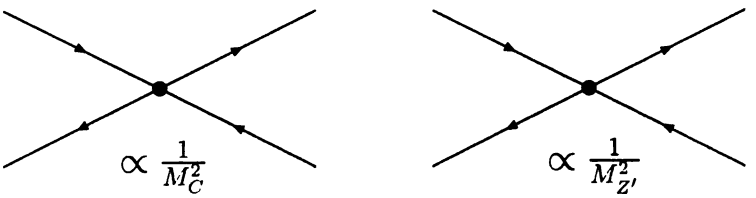

Figure 2.2. Topgluon and Z' exchange as effective four fermion interaction.

can be described by effective Lagrangians

$$\mathcal{L}_C = -\frac{2\pi}{M_C^2}\left[\sqrt{\kappa_3}\,\bar{\psi}_{III}\,\gamma_\mu\left(\frac{\lambda^a}{2}\right)\psi_{III} - \frac{\alpha_S}{\sqrt{\kappa_3}}\,\bar{\psi}_{I,II}\,\gamma_\mu\left(\frac{\lambda^a}{2}\right)\psi_{I,II}\right]^2 \tag{2.27}$$

$$\mathcal{L}_{Z'} = -\frac{2\pi}{M_{Z'}^2}\,\kappa_1\,\left(\bar{f}\gamma^\mu Y f\right)^2 \tag{2.28}$$

Note, that with the couplings as defined in eqns.(2.21) and (2.24), we can express the masses of the heavy gauge bosons in terms of p, Λ, κ_1 and κ_3:

$$M_C^2 = 4\pi\Lambda^2\frac{(\kappa_3+\alpha_S)^2}{\kappa_3}, \quad M_{Z'}^2 = \pi\,(p\Lambda)^2\,\frac{(\kappa_1+\alpha_Y)^2}{\kappa_1}. \tag{2.29}$$

2.2 Symmetry Breaking in the Electroweak Sector

In the previous section, we analyzed the symmetry breaking at the scale Λ and obtained in the $U(1)$-sector a massless field B'_μ coupling via the hypercharge $Y = Y_1 + Y_2$ as in the case of the unbroken standard model gauge group $U(1_Y)$. Additionally there is a massive vector field Z'_μ. Electroweak symmetry breaking is driven by two composite scalar fields ϕ_{TC} and φ_t, with the non-trivial vacuum expectation values of eq.(2.4).The effects of the extra ingredients on the breaking of the standard model gauge symmetry will be subject to the following analysis.

The Lagrangian describing the electroweak sector is given by

$$\mathcal{L} = \bar{\Psi} i \not{D} \Psi + \mathrm{tr}\left[\left(D_\mu \phi_{TC}\right)^\dagger D^\mu \phi_{TC}\right] + \mathrm{tr}\left[\left(D_\mu \varphi_t\right)^\dagger D^\mu \varphi_t\right] + \mathcal{L}_{Gauge}, \tag{2.30}$$

with

$$D_\mu = \partial_\mu + \imath g W_\mu^i \frac{\sigma^i}{2}_1 + \imath g' Y B'_\mu + \imath \left(g_{1(1)} \cos\phi \, Y_1 - g_{1(2)} \sin\phi \, Y_2 \right) Z'_\mu. \qquad (2.31)$$

Rewriting this in terms of the familiar fields, the photon A_μ, coupling via the conserved electric charge $Q = T_3 + Y$ and the Z boson, by rotating the W_μ^3 and the B'_μ fields by the weak mixing angle θ, gives

$$D^\mu = \partial^\mu + \imath \frac{g}{\sqrt{2}} W^+ \frac{\sigma^+}{2} + \imath \frac{g}{\sqrt{2}} W^- \frac{\sigma^-}{2} + \imath e Q A^\mu + \imath \frac{e}{\sin\theta\cos\theta} (T^3 - Q\sin^2\theta) Z^\mu$$
$$+ \imath \frac{e}{\cos\theta \sin\phi \cos\phi} (Y_1 - Y \sin^2\phi) Z'^\mu, \qquad (2.32)$$

where we have expressed the couplings in terms of the electric charge e and the rotation angles:

$$g = \frac{e}{\sin\theta}, \quad g'_2 = \frac{g'}{\cos\phi} = \frac{e}{\cos\theta\cos\phi}, \quad g'_1 = \frac{g'}{\sin\phi} = \frac{e}{\cos\theta\sin\phi} \qquad (2.33)$$

Evaluating the kinetic terms of the condensates in eq.(2.30), we find that the Z and Z' are no longer the appropriate superpositions of canonical gauge fields to represent mass eigenstates.

In order to have a more convenient notation at hand, we define $Y' \equiv Y_1 - \sin^2\phi Y$ and introduce the short handed notation

$$\langle \hat{O}_a \hat{O}_b \rangle \equiv \sum_i \langle \phi_i \rangle^\dagger \hat{O}_a^\dagger \hat{O}_b \langle \phi_i \rangle, \qquad (2.34)$$

where the sum runs over all condensates and $\hat{O}$ can denote any operator.

The proper mass eigenstates are obtained by diagonalizing the following mass matrix [4]

$$M_Z^2 = 2 \left(\frac{e}{\sin\theta\cos\theta} \right)^2 \begin{pmatrix} \langle T_3 T_3 \rangle & \frac{\sin\theta}{\sin\phi\cos\phi} \langle T_3 Y' \rangle \\ \frac{\sin\theta}{\sin\phi\cos\phi} \langle T_3 Y' \rangle & \frac{\sin^2\theta}{\sin^2\phi\cos^2\phi} \langle Y' Y' \rangle \end{pmatrix}. \qquad (2.35)$$

Evaluating the entries of the mass matrix gives for the upper diagonal entry:

$$\begin{aligned}\langle T_3 T_3\rangle &= \langle\phi_{TC}\rangle^\dagger T_3^\dagger T_3\langle\phi_{TC}\rangle + \langle\phi_t\rangle^\dagger T_3^\dagger T_3\langle\phi_t\rangle + \langle\Phi\rangle^\dagger T_3^\dagger \underbrace{T_3\langle\Phi\rangle}_{=0} \\ &= \frac{F_{TC}}{\sqrt{2}}(-\frac{1}{2})(-\frac{1}{2})\frac{F_{TC}}{\sqrt{2}} + \frac{f_t}{\sqrt{2}}(\frac{1}{2})(\frac{1}{2})\frac{f_t}{\sqrt{2}} \\ &= \frac{1}{8}(F_{TC}^2 + f_t^2) \equiv \frac{v^2}{8}. \end{aligned} \tag{2.36}$$

f_t denotes the decay constant of the top-condensate (in analogy to f_π, the pion decay constant in QCD). For the off-diagonal entries, we obtain

$$\langle T_3 Y'\rangle = \langle T_3 Y_1\rangle - \sin^2\phi\langle T_3 Y\rangle = \langle T_3 Y_1\rangle + \sin^2\phi\langle T_3 T_3\rangle, \tag{2.37}$$

where in the last step the conservation of electric charge has been employed: $Y = Q - T_3$ with $Q = 0 \Rightarrow Y = -T_3$. Then we can calculate

$$\langle T_3 Y_1\rangle = \langle\phi_{TC}\rangle^\dagger T_3^\dagger \underbrace{Y_1\langle\phi_{TC}\rangle}_{=0} + \langle\phi_t\rangle^\dagger T_3^\dagger Y_1\langle\phi_t\rangle = \frac{f_t}{\sqrt{2}}(\frac{1}{2})\underbrace{(Y_1^{tL} - Y_1^{tR})}_{-\frac{1}{2}}\frac{f_t}{\sqrt{2}} = -\frac{f_t^2}{8} \tag{2.38}$$

and conclude

$$\langle T_3 Y'\rangle = \frac{1}{8}\left(\sin^2\phi\, v^2 - f_t^2\right). \tag{2.39}$$

Finally, the lower diagonal entry gives

$$\begin{aligned}\langle Y'Y'\rangle &= \langle(Y_1 - \sin^2\phi Y)^2\rangle = \langle(Y_1 + \sin^2\phi T_3)^2\rangle \\ &= \langle Y_1 Y_1\rangle + 2\sin^2\phi\langle T_3 Y_1\rangle + \sin^4\phi\langle T_3 T_3\rangle \\ &= \langle\Phi\rangle^\dagger Y_1^\dagger Y_1\langle\Phi\rangle + \langle\phi_t\rangle^\dagger Y_1^\dagger Y_1\langle\phi_t\rangle - 2\sin^2\phi\frac{f_t^2}{8} + \sin^4\phi\frac{v^2}{8} \\ &= \frac{1}{8}\left(p^2\Lambda^2 + f_t^2 + \sin^4\phi v^2 - 2\sin^2\phi f_t^2\right). \end{aligned} \tag{2.40}$$

Factoring out

$$\left(\frac{e}{2\sin\theta\cos\theta}\right)^2 v^2 = M_{Z|SM}^2, \tag{2.41}$$

the mass matrix (eq.2.35) then takes the form

$$M_Z^2 = M_{Z|SM}^2 \begin{pmatrix} 1 & \alpha \\ \alpha & x \end{pmatrix}, \tag{2.42}$$

where α and x are given by

$$\begin{aligned} \alpha &\equiv \frac{\sin\theta}{\sin\phi\cos\phi}\frac{\langle T_3 Y'\rangle}{\langle T_3 T_3\rangle} = \frac{\sin\theta}{\sin\phi\cos\phi}\left(\sin^2\phi - \frac{f_t^2}{v^2}\right) \\ x &\equiv \frac{\sin^2\theta}{\sin^2\phi\cos^2\phi}\frac{\langle Y'Y'\rangle}{\langle T_3 T_3\rangle} \approx \frac{\sin^2\theta}{\sin^2\phi\cos^2\phi}\left(\frac{p\Lambda}{v}\right)^2 \end{aligned} \tag{2.43}$$

From diagonalizing the mass matrix, we obtain the eigenvalues

$$\begin{aligned} M_{Z/Z'}^2 &= \frac{1}{2}M_{Z|SM}^2\left(1 + x \mp (x-1)\sqrt{1 + \frac{4\alpha^2}{(x-1)^2}}\right) \\ &= M_{Z|SM}^2 \times \begin{cases} 1 - \frac{\alpha^2}{x} \\ x \end{cases}, \end{aligned} \tag{2.44}$$

to first order in $1/x$.

$$\Leftrightarrow \quad M_Z^2 = \frac{e^2v^2}{4\sin^2\theta\cos^2\theta}\left(1 - \frac{v^2}{p^2\Lambda^2}\left(\sin^2\phi - \frac{f_t^2}{v^2}\right)^2\right) \tag{2.45}$$

$$M_{Z'}^2 = \frac{e^2p^2\Lambda^2}{4\cos^2\theta\sin^2\phi\cos^2\phi}. \tag{2.46}$$

The corresponding eigenvectors take the form

$$Z_{new}^{\mu} = Z^{\mu} - \frac{\alpha}{x}Z'^{\mu} \tag{2.47}$$

$$Z_{new}'^{\mu} = \frac{\alpha}{x}Z^{\mu} + Z'^{\mu}. \tag{2.48}$$

From here on, we shall denote the new mass eigenstates simply as Z^{μ} and Z'^{μ}. The couplings of the new states to fermions can be read off directly from eq.(2.47) and

eq.(2.48)

$$g_Z = \frac{e}{\sin\theta\cos\theta}\left[T_3 - Q\sin^2\theta - \frac{v^2}{p^2\Lambda^2}\left(\sin^2\phi - \frac{f_t^2}{v^2}\right)\underbrace{\left(Y_1 - Y\sin^2\phi\right)}_{=Y\cos^2\phi}\right]$$

$$= \frac{e}{\sin\theta\cos\theta}\left[T_3\left(1 + \frac{v^2}{p^2\Lambda^2}\cos^2\phi\left(\sin^2\phi - \frac{f_t^2}{v^2}\right)\right)\right.$$

$$\left. - Q\left(\sin^2\theta + \frac{v^2}{p^2\Lambda^2}\cos^2\phi\left(\sin^2\phi - \frac{f_t^2}{v^2}\right)\right)\right] \tag{2.49}$$

$$g_{Z'} = \frac{e}{\cos\theta\sin\phi\cos\phi}Y\cos^2\phi = \frac{e}{\cos\theta}Y\cot\phi, \tag{2.50}$$

where we have used the fact, that all fermions transform only under $U(1)_1$. [3]

One should notice, that the mixing angle θ in the gauge couplings deviates from the weak mixing angle that appears in the standard model couplings. There are now several ways to define a weak mixing angle at tree-level. One of them is to define the mixing angle in terms of the three most precisely measured electroweak quantities α, G_F and M_Z

$$\sin^2\theta_Z\cos^2\theta_Z \equiv \frac{\pi\alpha}{\sqrt{2}G_F M_Z^2}, \tag{2.51}$$

corrections in $\sin\theta$ arise from the shift in the Z-mass (since the other constants remain the same as in the standard model). Plugging in the results from eq.(2.45) yields

$$\sin^2\theta_Z = \sin^2\theta + \frac{v^2}{p^2\Lambda^2}\frac{\sin^2\theta\cos^2\theta}{\cos^2\theta - \sin^2\theta}\left(\frac{F_{TC}^2}{v^2} - \cos^2\phi\right), \tag{2.52}$$

to second order in $\frac{v}{\Lambda}$. In this model the above definition deviates from the weak mixing angle defined by the ratio of the masses of the W and the Z bosons:

$$\cos^2\theta_W \equiv \left(\frac{M_W}{M_Z}\right)^2 = \cos^2\theta\left(1 + \left(\frac{v}{p\Lambda}\right)^2\left(\frac{F_{TC}^2}{v^2} - \cos^2\phi\right)^2\right). \tag{2.53}$$

[3]Working to this order, we obtain exactly the same result for the Z' mass and its coupling to the fermions as in the previous section.

Therefore, we have to be very careful, when calculating observables by shifting the couplings of the Z boson and the weak mixing angle in the standard model predictions, about the definition of the weak mixing angle.

2.3 The Nambu-Jona-Lasinio model

Let us now address the question how in the topcolor model the large top mass is created. The idea can be understood in terms of a useful toy-model, the NJL-model. We have a strong interaction $SU(3)_1$ which couples more strongly to the third generation of quarks than to the others. When $SU(3)_1 \times SU(3)_2$ breaks at the scale Λ, the top gluons acquire mass, according to eq.(2.12). At lower energies their interaction with fermions can be viewed as effective four fermion interaction (see Figure 2.1). As in the extended technicolor model in section 1.5, we notice that the Lagrangian from eq.(2.27) contains after a Fierz-rearrangement [3] terms of the form

$$\mathcal{L}_{NJL} = \frac{8\pi\kappa_3}{M_C^2}\left[\left(\bar{\psi}_L\, t_R\right)\left(\bar{t}_L\, \psi_R\right) + h.c.\right]. \tag{2.54}$$

We will refer to this as the NJL-Lagrangian. The NJL-model now assumes that the self-interaction of the top quarks is strong enough for a top-condensation, which leads to a mass creation as sketched in Figure 2.3. Self-consistently, one finds that the mass has to obey the following relation[4]

$$-\imath\, m = \frac{8\pi\kappa_3}{M_C^2}\int \frac{d^4k}{(2\pi)^4}\,\mathrm{tr}\left[\left(\frac{\imath}{\not k - m}\right)\frac{1}{2}\left(1+\gamma^5\right)\right] \times N_c \tag{2.55}$$

[4]Here one makes the rather strong dynamical assumption that the terms in eq.(2.54) are the only ones that contribute to the mass creation. We will therefore use the results that we obtain from the NJL-model only use for a qualitative analysis.

The trace gives a contribution of $4m$, since the trace of an odd number of γ-matrices vanishes. To carry out the integration, we rotate into Euclidean space

$$\begin{aligned} \imath m &= \frac{16\pi N_c \kappa_3}{M_C^2} m \int_0^{M_C^2} \frac{1}{(2\pi)^4} \frac{\imath\pi^2 \, k_E^2 \, dk_E^2}{-k_E^2 - m^2} \\ &= \imath \frac{N_c \kappa_3}{\pi} m \left(1 - \frac{m^2}{M_C^2} \log \left(\frac{M_C^2 + m^2}{m^2} \right) \right). \end{aligned} \tag{2.56}$$

From here we can see that we get constraints on κ_3 and Λ in order to make eq.(2.56) give us a finite positive solution for a top-mass (which will be treated as being equivalent to the formation of a top-condensate) according to

$$\kappa_3 - \frac{\pi}{N_c} = \frac{m^2}{M_C^2} \ln \frac{M_C^2}{m^2}, \tag{2.57}$$

where we have used that $M_C \gg m$. Eq.(2.57) is the so-called *gap-equation* for a dynamical fermion mass.

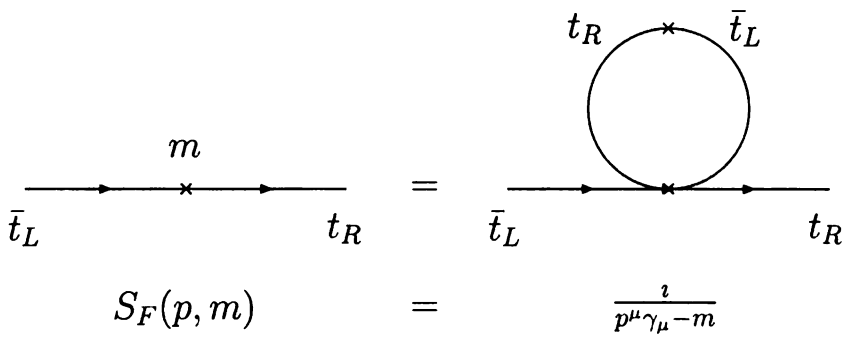

Figure 2.3. The process of dynamical mass creation as viewed in the NJL-model.

The above calculation lacks an explanation for the non-appearance of a bottom-quark condensation, since the top-gluons do not distinguish between top and bottom quarks. But we did not take into account the four fermion interaction due to exchange of a heavy Z' boson yet. Taking this interaction into account, we expect a constraint on κ_1, the effective coupling of the Z' to fermions. The process can then be understood as follows:

The coupling of the top-gluon κ_3 to t and b quarks has to be strong and very close to its critical value at which a top- and bottom-quark condensation occurs. Then the self-interaction due to Z'-exchange, which depends on the hyperpercharge Y and hence distinguishes between top- and bottom-quarks, tilts the total self-interaction to be either strong enough to create a condensate or not.

The calculation taking the Z' into account is analogous to the steps shown above, albeit more complicated, and we modified the results from [17] to our model. The resulting gap-equation for our model is:

$$\begin{aligned} m_f = G_1 \frac{m_f M_{Z'}^2}{8\pi^2}\left[1 - \left(\frac{m_f}{M_{Z'}}\right)^2 \ln\left(\frac{M_{Z'}^2}{m_f^2}\right)\right] \\ + G_3 \frac{3 m_f M_C^2}{8\pi^2}\left[1 - \left(\frac{m_f}{M_C}\right)^2 \ln\left(\frac{M_C^2}{m_f^2}\right)\right], \end{aligned} \tag{2.58}$$

where

$$G_1 = \frac{8\pi}{M_{Z'}^2}\kappa_1 Y_L^f Y_R^f \qquad \text{for all fermions,} \tag{2.59}$$

$$G_3 = 0 \qquad \text{for leptons,} \tag{2.60}$$

$$= \frac{4\pi\alpha_s^2}{M_C^2 \kappa_3} \qquad \text{for quark gen. I,II,} \tag{2.61}$$

$$= \frac{4\pi}{M_C^2}\kappa_3 \qquad \text{for quark gen. III.} \tag{2.62}$$

This model does not take into account the unbroken gauge interactions, which can contribute to the condensation as well. Including the appropriate correction terms yields according to [17] the *gauged* gap equation

$$\begin{aligned} m_f\left(1 - \frac{2}{\pi}\alpha_S - \frac{6}{\pi}Y_L^f Y_R^f \alpha_Y\right) = G_1 \frac{m_f M_{Z'}^2}{8\pi^2}\left[1 - \left(\frac{m_f}{M_{Z'}}\right)^2 \ln\left(\frac{M_{Z'}^2}{m_f^2}\right)\right] \\ + G_3 \frac{3 m_f M_C^2}{8\pi^2}\left[1 - \left(\frac{m_f}{M_C}\right)^2 \ln\left(\frac{M_C^2}{m_f^2}\right)\right] \end{aligned} \tag{2.63}$$

A positive solution for a fermion mass to the gap-equation is taken to be equivalent to the occurrence of a condensation of the respective fermion. We will choose the couplings such that we obtain a top-, but no bottom-condensate.

The top-condensate $\langle \bar{t}t \rangle \neq 0$ breaks chiral symmetry which makes three top-pions appear in the spectrum.[5] Their decay constant can be estimated using the Pagels-Stokar relation [12] to be

$$\frac{f_t^2}{2} = m_t^2 \frac{N_c}{16\pi^2} \ln\left(\frac{\Lambda^2}{m_t^2}\right). \tag{2.64}$$

[5]Since there is no reliable estimation of their masses, we just have to assume that they are heavy enough not to give rise to potentially dangerous effects [12].

Chapter 3

Theoretical Constraints

In this chapter we shall investigate how the parameters have to be chosen, so that the model can provide the required generation of the top mass. We will also briefly discuss the Landau-pole of the $U(1)_1$ group and how the parameter space gets constrained by the requirement that we want the theory to be valid up to high scales.

3.1 Constraints From the Gap Equation

Inserting the masses of the heavy gauge bosons from eq.(2.29) into the gap equation and assuming $\Lambda \gg m_f$, yields

$$m_f \left(1 - \frac{2}{\pi}\alpha_S - \frac{6}{\pi}Y_L^f Y_R^f \alpha_Y\right) = \frac{m_f}{8\pi^2}\left(M_{Z'}^2 G_1 + 3M_C^2 G_3\right) \tag{3.1}$$

In order to obtain a non trivial, positive solution for m_f in eq.(2.63), i.e. a fermion condensate $\langle \bar{f} f \rangle \neq 0$,

$$\frac{1}{8\pi^2}\left(M_{Z'} G_1 + 3M_C G_3\right) \geq 1 - \frac{2}{\pi}\alpha_S - \frac{6}{\pi}Y_L^f Y_R^f \alpha_Y \tag{3.2}$$

must hold.

Since we only want top-condensation to occur, we have to make sure that there is a

solution for the top quark-mass, but none for the other fermions.[1] The three strongest bounds come from the following set of inequalities[2]:

$$\begin{aligned}
\langle \bar{t}t \rangle \neq 0, \quad \text{if} \quad & \kappa_3 + \frac{2}{27}\kappa_1 \geq \frac{2\pi}{3} - \frac{4}{3}\alpha_S - \frac{4}{9}\alpha_Y \\
\langle \bar{b}b \rangle = 0, \quad \text{if} \quad & \kappa_3 - \frac{1}{27}\kappa_1 \leq \frac{2\pi}{3} - \frac{4}{3}\alpha_S + \frac{2}{9}\alpha_Y \\
\langle \bar{\tau}\tau \rangle = 0, \quad \text{if} \quad & \kappa_1 \leq 2\pi - 6\alpha_Y,
\end{aligned} \tag{3.3}$$

which are plotted in Figure 3.1.

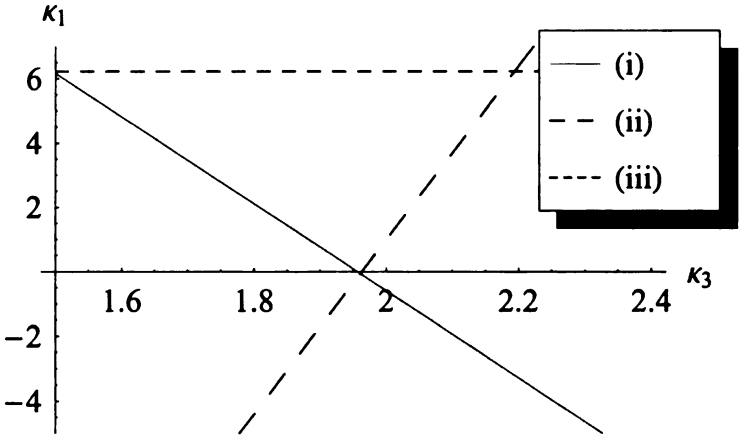

Figure 3.1. The triangle of allowed values for κ_1 and κ_3.

Above the line (i) is the area, where $\langle \bar{t}t \rangle \neq 0$; (iii) is the upper limit, for non-appearance of τ condensation and (ii) the lower bound from $\langle \bar{b}b \rangle = 0$.

Note, that curves (ii) and (iii) remain the valid limits for the $\langle \bar{b}b \rangle = \langle \bar{\tau}\tau \rangle = 0$ regardless of the size of the scale Λ. Since we do not want to have any mass being created by condensation of b-quarks or τ's, the approximation that leads to eq.(3.1)

[1]We do not know the exact value of the part of the top mass that has to be generated via this mechanism, since we also expect a small contribution of a few GeV from the Extended Technicolor sector. But fortunately our analysis turns out not to be sensitive to small deviations in the top mass that comes from top-condensation.

[2]Even though the last inequality follows from eq.(3.2), the formation of a τ-condensate does not fit into our picture of the mass generation, since the leptons do not couple to the strongly interacting sector. During our following analysis it will turn out that this region of the parameter space will not be of interst.

is always valid for $m_f \to 0 + \epsilon$. On the other hand the limit for top-condensation becomes a single line in the $\kappa_3 - \kappa_1$ plane, if we assume the condensation to happen at a particular scale. In Figure 3.2 the lines that represent the allowed parameter space for top-condensation at a particular choice for Λ are plotted for different values of Λ, assuming the hypercharge p of the condensate that forms at that scale to be one.

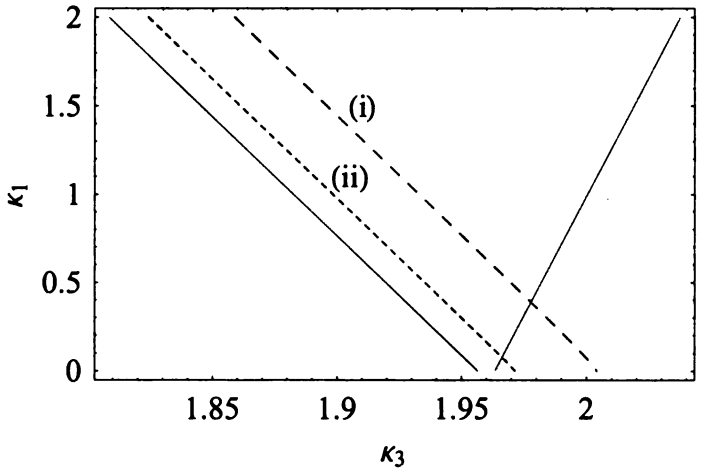

Figure 3.2. The curves (i) and (ii) show the allowed parameter space in the $\kappa_3 - \kappa_1$ plane for a scale $\Lambda = 500\,\text{GeV}$, $1000\,\text{GeV}$ respectively. The solid lines represent the tip of the gap triangle in Figure 3.1.

Of course the values for Λ are always within a certain interval, but on can see that if the scale is forced to be higher than 1 TeV, the parameter space will be very narrow.[3]

3.2 The Landau-Pole

In loop calculations in gauge theories one generally encounters infinities that force us to think about the meaning of the coupling constants and masses appearing in the Lagrangian. The procedure of redefining the constants in a sensible way, such that

[3]The line that would belong to $\Lambda = 10$ TeV is already so close to the line from top condensation at an infinite scale that the resolution of the plots was not high enough to separate them.

those infinities cancel, is called renormalization. According to the standard literature (e.g.[15]), the coupling constants become dependent on the momentum transfer in the loops ("running couplings"). For Abelian gauge theories like QED, the strength of the coupling increases with energy, whereas in non-Abelian gauge theories like QCD the coupling constant is strong at low energies and converges to a small value at high energies ("asymptotic freedom"). The Landau-Pole denotes the scale at which the running coupling constant of an Abelian theory becomes infinitely strong, i.e. the physics at this energy cannot be described by that theory any more.

In the model, that we are investigating, we expect the coupling of the $U(1)_1$ group to exhibit such a running behavior. [4]

In analogy to QED, the running of the coupling constant

$$\alpha_{Y_1} \equiv \frac{g_{1(1)}^2}{4\pi} = \alpha_Y + \kappa_1 \tag{3.4}$$

is given by

$$\alpha_{Y_1}\Big|_{\Lambda_H} = \frac{\alpha_{Y_1}\Big|_{\Lambda}}{1 - \alpha_{Y_1}\Big|_{\Lambda} \frac{C}{3\pi} \ln\left(\frac{\Lambda_H}{\Lambda}\right)}, \tag{3.5}$$

where C denotes the sum over the squared $U(1)_1$-charges of all particles contributing to the self-energy of the $U(1)_1$ gauge boson. Taking all standard model fermions in a chiral representation into account, we obtain $C = 5$. Inserting eq.(3.4) into (3.5) and assuming that $\alpha_Y(\Lambda) \approx \alpha_Y(M_Z) = \alpha(M_Z)/\cos\theta$, we obtain the ratio of Λ_H/Λ as a function of κ_1.

[4] Since there are no fermions transforming under the second $U(1)$ group, there are no interactions that could cause a running behavior.

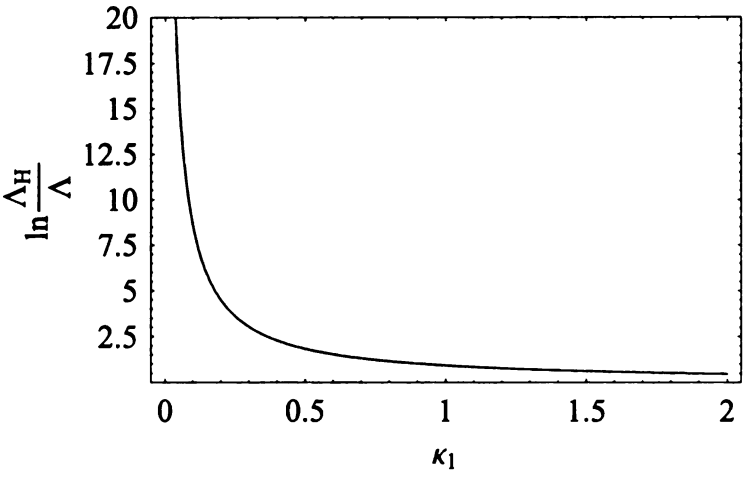

Figure 3.3. $\ln(\Lambda_H/\Lambda)$ as a function of κ_1.

As one can see from Figure 3.3, κ_1 has to be very small, if we want our theory to be valid up to a very high scale.

Chapter 4

First Constraints from Existing Data

Our model shifts the predictions of the standard model for well measured observables. We shall investigate in this and the following chapter how the parameters of our model are constraint by the requirement that our predictions for observables are in agreement with current experimental data.

4.1 Flavor Changing Neutral Currents (FCNC)

The fermion fields appearing in the effective Lagrangian eq.(2.27) are in their gauge eigenstates. As the top-gluons single out the third quark generation, there can occur a further unknown mixing among the mass eigenstates of up- and down-type quarks respectively.

For a first estimation of how this mixing limits the free parameters of our model, we assume that only the left handed down-type quarks mix, according to the CKM-mechanism from the electroweak theory. This yields FCNC at tree-level according

to:

$$\begin{aligned}\mathcal{L} = &-\frac{2\pi}{M_C^2}\Big[\kappa_3\Big(\bar{b}'\gamma^\mu\frac{\lambda^a}{2}b'\Big)^2+\frac{{\alpha_s}^2}{\kappa_3}\Big(\bar{D}_i'\gamma^\mu\frac{\lambda^a}{2}D_i'\Big)^2\\ &-2\alpha_s\Big(\bar{D}_i'\gamma^\mu\frac{\lambda^a}{2}D_i'\Big)\Big(\bar{b}'\gamma^\mu\frac{\lambda^a}{2}b'\Big)\Big]\\ = &-\frac{2\pi}{{M_C}^2}\Big[\kappa_3\Big(\big(V_{3i}^\dagger V_{j3}\big)\bar{B}_i\gamma^\mu\frac{\lambda^a}{2}B_j\Big)^2+\frac{{\alpha_s}^2}{\kappa_3}\Big(\big(V_{ji}^\dagger V_{ik}\big)\bar{B}_j\gamma^\mu\frac{\lambda^a}{2}B_k\Big)^2\\ &-2\alpha_s\Big(\big(V_{ji}^\dagger V_{ik}\big)\bar{B}_j\gamma^\mu\frac{\lambda^a}{2}B_k\Big)\Big(\big(V_{3i}^\dagger V_{j3}\big)\bar{B}_i\gamma^\mu\frac{\lambda^a}{2}B_j\Big)\Big],\end{aligned} \tag{4.1}$$

where the primed fields denote the gauge eigenstates and the unprimed, the mass eigenstates, which are obtained by rotating the gauge eigenstates with V. Further, I used the abbreviations $D = (d, s)^T$ and $B = (d, s, b)^T$.

In order to find the constraints on the free parameters of our model, we compare the FCNC arising from top gluon exchange to the standard model prediction.

4.1.1 FCNC in $\bar{K}^0 - K^0$ systems

In the standard model, FCNC arise at loop-level from interactions as displayed in the box diagrams in Figure 4.1.

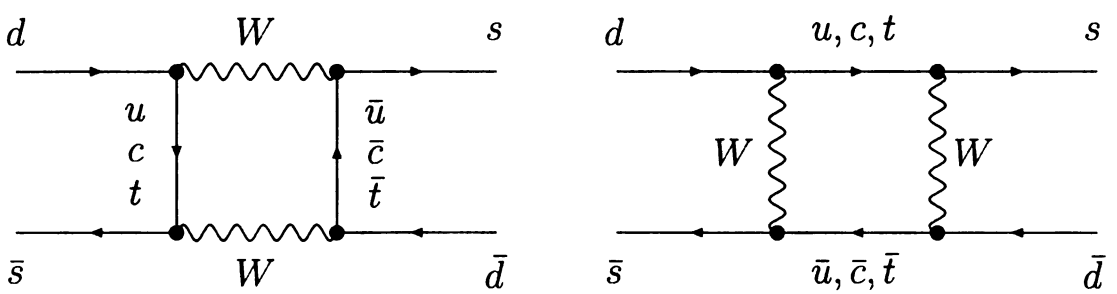

Figure 4.1. Box diagrams of W bosons causing FCNC in the $\bar{K}^0 - K^0$ system.

This interaction can be described in terms of an effective Lagrangian of the form [3]

$$L_{eff\ SM} = -\Omega_{SM}\big(\bar{d}_L\gamma^\mu s_L\big)^2, \tag{4.2}$$

where

$$\Omega_{SM} := -\frac{G_F}{\sqrt{2}}\frac{\alpha}{16\pi}\left(\frac{1}{M_W \sin\theta_w}\right)^2 \sum_i V_{i2}V_{i1}^* m_i \,. \tag{4.3}$$

The corresponding physical observable would be the $\bar{K}^0 - K^0$ mass splitting, but for our purposes it is sufficient to just compare the factors Ω in the Lagrangian. The Lagrangian yielding the $\Delta S = 2$ neutral currents at tree-level in our model reads:[1]

$$\begin{aligned}\mathcal{L}_C = -\frac{2\pi}{{M_C}^2}\Big(\kappa_3\left(V_{13}^\dagger V_{32}\right)^2 + \frac{{\alpha_s}^2}{\kappa_3}\Big[\left(V_{11}^\dagger V_{12}\right)^2 + \left(V_{12}^\dagger V_{22}\right)^2 + 2\left(V_{11}^\dagger V_{12} V_{12}^\dagger V_{22}\right)\Big] \\ -2\alpha_s\Big[\left(V_{11}^\dagger V_{12} V_{13}^\dagger V_{32} + V_{12}^\dagger V_{22} V_{13}^\dagger V_{32}\right)\Big]\Big)\left(\bar{d}_L\gamma^\mu\frac{\lambda^a}{2}s_L\right)^2 .\end{aligned} \tag{4.4}$$

In order to compare the factors in the Lagrangians, we have to bring the currents in eq.(4.4) to the form of the current of the effective standard model Lagrangian eq.(4.2). We sum over the indices of the Gell-Mann matrices λ^a and employ the relation

$$\sum_a \left(\frac{\lambda^a}{2}\right)_{\alpha\beta}\left(\frac{\lambda^a}{2}\right)_{\gamma\delta} = \frac{1}{2}\left(\delta_{\alpha\delta}\delta_{\beta\gamma} - \frac{1}{3}\delta_{\alpha\beta}\delta_{\gamma\delta}\right) \tag{4.5}$$

This yields a term of the shape

$$\left(\bar{d}_{L\alpha}\gamma^\mu s_{L\beta}\right)\left(\bar{d}_{L\beta}\gamma_\mu s_{L\alpha}\right) = (-)(-)\left(\bar{d}_L\gamma^\mu s_L\right)^2, \tag{4.6}$$

where the first minus sign comes from a Fierz-rearrangement and the second one from interchanging Grassmann valued fermion fields. Plugging this in the Lagrangian

[1]Note, that for gauge bosons that couple equally to all fermion generations, the couplings could be factored out and the sum over the matrix elements would give 1, since the mixing matrix has to be unitary. In that case there is no residual flavor changing neutral current.

eq.(4.4) and comparing the factors, demanding

$$\Omega_{SM} > -\frac{2\pi}{{M_C}^2}\left(\kappa_3\left(V_{13}^{\dagger}V_{32}\right)^2+\frac{{\alpha_s}^2}{\kappa_3}\left[\left(V_{11}^{\dagger}V_{12}\right)^2+\left(V_{12}^{\dagger}V_{22}\right)^2+2\left(V_{11}^{\dagger}V_{12}V_{12}^{\dagger}V_{22}\right)\right]\right.$$
$$\left.-2\alpha_s\left[\left(V_{11}^{\dagger}V_{12}V_{13}^{\dagger}V_{32}+V_{12}^{\dagger}V_{22}V_{13}^{\dagger}V_{32}\right)\right]\right), \tag{4.7}$$

yields the constraints for κ_3 and M_C shown in Figure (4.2).

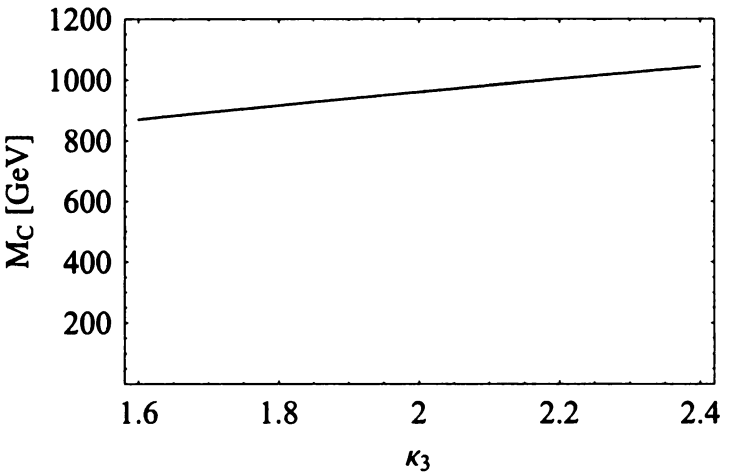

Figure 4.2. Lower bound for (κ_3, M_C) from FCNC in $\bar{K}^0 - K^0$ systems

4.1.2 FCNC in $\bar{B}^0 - B^0$ systems

The same procedure can be repeated for $\bar{B}^0 - B^0$ systems, where we obtain similar constraints from the mass shift in B_d^0 or B_s^0 mesons. The corresponding graph is shown in Figure(4.3).

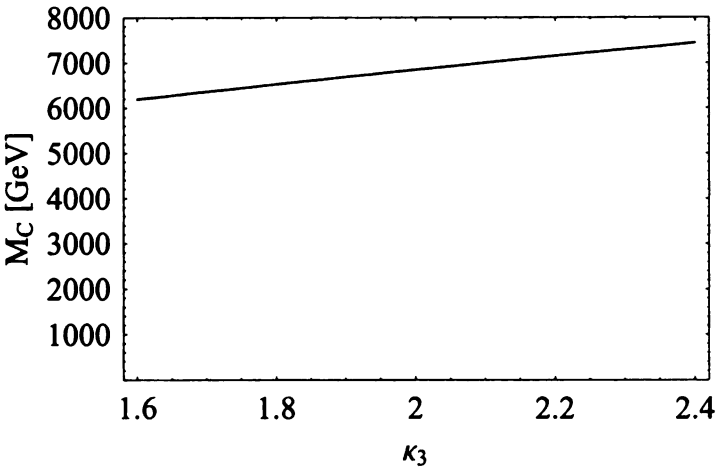

Figure 4.3. Lower bound for M_C as a function in κ_3 from FCNC in B_s^0-Meson systems

One can see directly from Figure 4.3 that this constraint is stronger than the one from the kaon sector. From the gap triangle in Figure 3.1, we have $\kappa_3 \approx 2$, which yields a lower bound on the top gluon mass of approximately 6 TeV.

4.2 Constraints on effective four-fermion couplings

Data from LEP2 puts upper limits on the coupling in effective four fermion contact interactions. The data is presented in the following form:

If the Lagrangian has the form

$$\mathcal{L}_{eff} = \pm \frac{g^2}{2\Lambda_{LL}^{\pm\,2}} \left(\bar{\psi}_L \gamma_\mu \psi_L\right) \left(\bar{\psi}_L \gamma^\mu \psi_L\right), \tag{4.8}$$

with $\frac{g^2}{4\pi} \equiv 1$, then LEP2 data gives lower limits for $\Lambda_{LL}^{\pm}$ or upper limits for the overall coefficient in the Lagrangian.

This becomes interesting for us, if we look at the effective four-fermion interaction, due to Z' exchange:

$$\mathcal{L}_{Z'} = -\frac{2\pi}{{M_{Z'}}^2}\kappa_1 \left(\bar{f}_i \gamma^\mu Y f_i\right)\left(\bar{f}_j \gamma^\mu Y f_j\right). \tag{4.9}$$

Even though one might expect the most restrictive constraint for κ_1 and $M_{Z'}$ to follow from leptonic contact interactions $(eeee)$ or $(ee\mu\mu)$, it arises from the contact interaction $(eeuu)$, for which the factor $\lambda_{LL}^{+} = 23.3$ TeV is the largest. [2]

The graph in Figure 4.4 shows the lower limit for the allowed region for $(\kappa_1, M_{Z'})$.

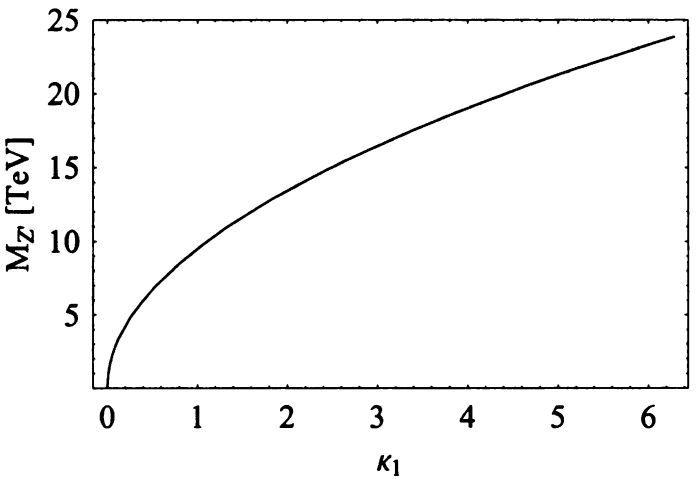

Figure 4.4. Lower limits for κ_1 and $M_{Z'}$ from comparison with LEP2 data.

In order to keep $M_{Z'}$ on the order of a few TeV, κ_1 is restricted to be smaller than 1.

[2]Notice, that, even though our Lagrangian had initially an overall minus sign, we have to use the value for Λ according to an overall positive Lagrangian, as the hypercharge eigenvalues for electrons and quarks have opposite signs.

Chapter 5

Constraints from electroweak precision data

In this chapter we will investigate the bounds on our parameter space from electroweak precision measurements. At first we present our fit to the LEP1 data given in [7]. In the second section we compare our results to the fit by Barbieri *et al* [2] to data from LEP1-, LEP2-, low energy-experiments.

5.1 A Fit to LEP1 data

In order to find constraints on the parameter space of the model, we have to derive expressions for the observables. These can be obtained at tree level by shifting the coupling of the Z boson and the weak mixing angle in the standard model observables according to eqns.(2.49) and (2.52). The observables are then functions of the very well measured quantities M_Z, α and G_F as well as the free parameters in the electroweak sector $\cos\phi$ and $p\Lambda$. Note that f_t and hence F_{TC} are already determined in terms of these parameters according to eqns.(2.64) and (2.36).

Since we expect $p\Lambda \gg v \approx 246$ GeV, we expand to second order in $\frac{v}{p\Lambda}$. Every

observable then takes the form

$$\mathcal{O}^i = \mathcal{O}^i_{SM} + \delta\mathcal{O}^i(\cos\phi) \times \frac{v^2}{p^2\Lambda^2}, \tag{5.1}$$

where $\delta\mathcal{O}^i(\cos\phi)$ is a polynomial in $\cos\phi$. From this we see, that in the limit $\Lambda \to \infty$ and $\cos\phi \to 0$, we approach the standard model. $\mathcal{O}^i_{SM}$ represents the tree-level standard model value for the observable written in terms of $\sin\theta_Z$.

In order to get bounds on the free parameters, we have to compare our expression for $\mathcal{O}^i$ to the experimental value $\mathcal{O}^i_{exp}$:

$$\mathcal{O}^i_{exp} \pm \sigma\mathcal{O}^i_{exp} \gtrless \mathcal{O}^i_{SM} + \delta\mathcal{O}^i(\cos\phi) \times \frac{v^2}{p^2\Lambda^2} \tag{5.2}$$

We expect that the new effects coming from our model are of the same order as one-loop corrections to the standard model. To make sure that we do not mistake standard model one-loop corrections for new physics, we replace $\mathcal{O}^i_{SM}$ in eq.(5.2) by the best-fit standard model one-loop value for the corresponding observable. We obtain those values using the program ZFITTER [1]. We used the sample program given in [1] and updated the subroutine which is in charge of the initialization. The values we used as input parameters are listed in Table 5.1.

The one-loop correction to the standard model involves a Higgs particle loop, which strongly depends on the Higgs mass. The particle in our model corresponding to the Higgs would be the particle that unitarizes the W scattering, which is in this class of models assumed to be the Technicolor-analog to the QCD-ρ. Its mass can be estimated by upscaling the QCD-ρ mass to be of the order of a TeV.

In order to see how the mass of the particle that plays the role of the Higgs in the loop-calculations affects our results, we performed the fit for two different input parameters $m_H = 800$ geV and $m_H = 1.5$ TeV.

M_Z [GeV]	$\alpha^{-1}(M_Z)$	α_S	m_t [GeV]	m_H [Gev]
91.1876	128.887	0.117	174.2	800/1500

Table 5.1. The input parameters we used in ZFITTER.

To combine the constraints from measurements of several observables, one has to perform a *least-squares* fit, i.e. the best fit values are obtained by minimizing

$$\chi^2(\cos\phi, p\Lambda) = \sum_{i,j} \left(\mathcal{O}^i_{exp} - \mathcal{O}^i_{SM} - \delta\mathcal{O}^i(\cos\phi) \times \left(\frac{v}{p\Lambda}\right)^2 \right) \times (\sigma\rho\sigma)^{-1}_{ij} \left(\mathcal{O}^j_{exp} - \mathcal{O}^j_{SM} - \delta\mathcal{O}^j(\cos\phi) \times \left(\frac{v}{p\Lambda}\right)^2 \right), \tag{5.3}$$

where ρ denotes the correlation matrix of the observables and σ is the diagonal matrix containing their standard deviations. The allowed parameter space is obtained, by requiring that $\Delta\chi^2 = \chi^2 - \chi^2_{\text{min}}$ does not exceed a certain value, associated with the confidence level and the number of fit parameters. We will work at a 2σ confidence level and have two fit parameters $p\Lambda$ and $\cos\phi$, which yields according to [8] $6.17 \geq \Delta\chi^2$.

Since we obtained the first bounds on our parameter space from the gap equation (3.2), we want in the end to translate our constraints back into the κ_3-κ_1 plane.[1] Comparing eq.(2.18) and eq.(2.21) yields

$$\cos^2\phi = \frac{\kappa_1}{\kappa_1 + \alpha_Y}. \tag{5.4}$$

In order to impose limits on κ_3, we use the gauged gap equation for the desired top

[1]The results of this part of the analysis have a rather qualitative character, since one should not assume that the self-consistent ansatz of the NJL-approximation holds to such high accuracy.

mass

$$1-\frac{2}{9\pi}\alpha_S-\frac{2}{3\pi}\alpha_Y=\frac{1}{4\pi}Y_L^tY_R^t\kappa_1\left[1-\left(\frac{m_t}{M_{Z'}}\right)^2\log\left(\frac{M_{Z'}^2}{m_t^2}\right)\right]+\frac{3}{2\pi}\kappa_3\left[1-\left(\frac{m_t}{M_C}\right)^2\log\left(\frac{M_C^2}{m_t^2}\right)\right] \tag{5.5}$$

Inserting the relation for the heavy gauge boson masses from eq.(2.29), one can see that eq.(5.5) depends only on the free parameters Λ, κ_1, κ_3 and p

$$1-\frac{2}{9\pi}\alpha_S-\frac{2}{3\pi}\alpha_Y=\frac{1}{36\pi}\kappa_1\left[1-\left(\frac{m_t^2\kappa_1}{4\pi(p\Lambda)^2(\kappa_1+\alpha_Y)^2}\right)\log\left(\frac{4\pi(p\Lambda)^2(\kappa_1+\alpha_Y)^2}{m_t^2\kappa_1}\right)\right]+\frac{3}{2\pi}\kappa_3\left[1-\left(\frac{p^2m_t^2\kappa_3}{4\pi(p\Lambda)^2(\kappa_3+\alpha_S)^2}\right)\log\left(\frac{4\pi(p\Lambda)^2(\kappa_3+\alpha_S)^2}{p^2m_t^2\kappa_3}\right)\right]. \tag{5.6}$$

In order to eliminate $p\Lambda$ we solve eq.(5.2) for $p\Lambda$ and obtain $p\Lambda$ as a function of κ_1. Inserting this into eq.(5.6) enables us to translate the constraint into the $\kappa_3-\kappa_1$ plane, with a dependency on the parameter p.

Recall that p denotes the absolute value of hypercharge assigned to the condensate that drives the first symmetry breaking. It is assumed that p is of the order of one, but we shall demonstrate how different choices of p affect our results.

According to eq.(2.53), the shift in the W mass is given by

$$\begin{aligned}M_W^2 &= M_Z^2\cos^2\theta\left(1+\left(\frac{v}{p\Lambda}\right)^2\left(\frac{F_{TC}^2}{v^2}-\cos^2\phi\right)^2\right)\\ &= \underbrace{M_Z^2\cos^2\theta_Z}_{M_W^2|SM}+\underbrace{M_Z^2\left(\frac{v}{p\Lambda}\right)^2\frac{\cos^4\theta_Z}{cos^2\theta_Z-\sin^2\theta_Z}\left(\frac{F_{TC}^2}{v^2}-\cos^2\phi\right)^2}_{=\left(\frac{v}{p\Lambda}\right)^2\delta M_W^2},\end{aligned} \tag{5.7}$$

where in the last step we have used eq.(2.52) to express $\cos^2\theta$ in terms of $\cos^2\theta_Z$ and expanded to second order in $v/p\Lambda$. As outlined in the previous section, we replace

$M^2_{W|SM}$ by the best-fit one-loop value, obtained by running ZFITTER (see Table 5.2).

The partial decay width of the Z boson into a fermion-antifermion pair $(\bar{f}f)$ is given by (see e.g. [3]):

$$\Gamma(Z \to \bar{f}f) = \frac{M_Z}{24\pi}(g_L^{f\,2} + g_R^{f\,2}). \tag{5.8}$$

Using the expression for the new Z-coupling from eq.(2.49), one obtains

$$\begin{aligned}\Gamma(Z \to \bar{f}f) =& \frac{M_Z}{24\pi}\frac{e^2}{\sin^2\theta\cos^2\theta} \\ &\times \left[\left(T_{3L}^f \cos^2\theta - Y_L^f\left(\sin^2\theta + \frac{v^2}{p^2\Lambda^2}\cos^2\phi\left(\sin^2\phi - \frac{f_t^2}{v^2}\right)\right)\right)^2\right. \\ &\left. + \left(Y_L^f\left(\sin^2\theta + \frac{v^2}{p^2\Lambda^2}\cos^2\phi\left(\sin^2\phi - \frac{f_t^2}{v^2}\right)\right)\right)^2\right]\end{aligned} \tag{5.9}$$

Rewriting this in terms of θ_Z using the result from eq.(2.52) and expanding to second order in $\frac{v}{p\Lambda}$ yields an expression of the form of eq.(5.1)

$$\Gamma(Z \to \bar{f}f) = \Gamma(Z \to \bar{f}f)_{SM|\text{tree level}} + \delta\Gamma(Z \to \bar{f}f) \times \frac{v^2}{p^2\Lambda^2} \tag{5.10}$$

Neglecting the small contribution from the Z decaying into other gauge bosons and hadronic states we can write the decay width into hadrons as

$$\Gamma_{Z\to\text{had}} = \sum_{f=u,d,s,c,b} N_c\Gamma(Z \to \bar{f}f), \tag{5.11}$$

where $N_c = 3$ is the color factor.[2] $\Gamma_{Z\to\text{inv}}$ is given by summing eq.(5.10) over all neutrinos. The total Z-boson decay width was calculated by summing all partial decay-widths into fermion-antifermion pairs (excluding the top quark).

[2]The decay into a $t\bar{t}$ pair is kinematically impossible at the Z pole, since the top mass exceeds the center of mass energy by far.

The experimental results in [7] further include values for the *pseudo*-observables as defined in the following: The hadronic cross section of the Z boson σ_{had} is given by

$$\sigma_{\text{had}} = \frac{12\pi}{M_Z^2} \frac{\Gamma_{Z\to e\bar{e}}\,\Gamma_{Z\to\text{had}}}{\Gamma_{Z\text{ tot}}}\,. \tag{5.12}$$

The *branching ratios* into quarks and leptons are defined as

$$R_q \equiv \frac{\Gamma_{Z\to q\bar{q}}}{\Gamma_{Z\to\text{had}}}\,, \qquad R_l \equiv \frac{\Gamma_{Z\to\text{had}}}{\Gamma_{Z\to l\bar{l}}}. \tag{5.13}$$

Futher, the *left-right* and *forward-backward* asymmetry parameters are introduced as

$$A_{LR}^f \equiv \frac{\sigma_L^f - \sigma_R^f}{\sigma_L^f + \sigma_R^f}\frac{1}{\langle|P_e|\rangle}, \quad A_{FB}^f \equiv \frac{\sigma_F^f - \sigma_B^f}{\sigma_F^f + \sigma_B^f}\,, \tag{5.14}$$

where in the first expression $\langle|P_e|\rangle$ denotes the polarization of the initial state electrons. Important for us is that in the standard model they can be conveniently rewritten in terms of another asymmetry parameter, which is only a function of the coupling of the Z boson to fermions

$$\mathcal{A}_f \equiv \frac{g_{fL}^2 - g_{fR}^2}{g_{fL}^2 + g_{fR}^2}\,. \tag{5.15}$$

With the above definition we obtain

$$A_{LR}^f = \mathcal{A}_f \qquad \text{and} \qquad A_{FB}^f = \frac{3}{4}\mathcal{A}_e\,\mathcal{A}_f\,. \tag{5.16}$$

In order to calculate the predictions for the pseudo-observables in our model, we again replace the Z-coupling by the shifted expression from eq.(2.49) and further express $\sin\theta$ by $\sin\theta_Z$ according to eq.(2.52). We expand to second order in $\frac{v}{p\Lambda}$ and replace the zeroth order term by the standard model prediction at one-loop level from ZFITTER[1] listed in Table 5.2. In order to obtain values for the asymmetry parameters, the ZFITTER-based program Smatasi [14] was used.[3]

[3] At this point, the author would like to thank his fellow student Michael Floßdorf who was responsible for the complicated but in the end successful installation of this program, which enabled us to perform this improved fit.

Since in our model the hypercharge sector is flavor-universal, we used the values from [7] which were calculated under the assumption of lepton-universality. The ZFITTER values for the flavor-universal observables $\mathcal{O}^l$ were calculated by averaging over the values for $\mathcal{O}^e$, $\mathcal{O}^\mu$, and $\mathcal{O}^\tau$. In the fitting procedure we minimized the χ^2-function in eq.(5.3) under the conditions $p\Lambda, \kappa_1 > 0$. The experimental values and their errors are displayed together with the results of our fit (for $m_H = 800$ GeV) in Figure 5.1. The correlation matrices for the observables can be found in Table 5.3 at the end of this section. In the "Fit"-column the predictions of our model for the observables using the best-fit values for the fit parameters $p\Lambda$ and κ_1 are listed. The "Pulls" quantify how much the prediction of our model deviates from the experimental value in units of its standard deviation.

Experimental Value	Fit	Pull
Γ_Z= (2.4952±0.0023) GeV	2.4978 GeV	
σ_{had}= (41.541±0.037) nb	41.485 nb	
R_l= 20.767±0.025	20.733	
A^l_{FB}= 0.0171±0.0010	0.0161	
P_τ= 0.1465±0.0033	0.1465	
A^l_{LR}(SLD)= 0.1513±0.0021	0.1465	
R_b= 0.21629±0.00066	0.2160	
R_c= 0.1721±0.0030	0.1723	
A^b_{FB}= 0.0992±0.0016	0.1027	
A^c_{FB}= 0.0707±0.0035	0.0733	
A^b_{LR}= 0.923±0.020	0.935	
A^c_{LR}= 0.670±0.027	0.668	
M_W= (80.403±0.029) GeV	80.402 GeV	
		0 1 2 3
χ^2_{min}=15.772 at $\langle p\Lambda \rangle$ = 4.038 TeV, $\langle \kappa_1 \rangle$ = 0		

Figure 5.1. The first column shows experimental values from [7] for the set of observables we used to fit the predictions of our model to. In the second column the best-fit results for our model are listed and the graph on the right-hand side shows the pulls for each observable. In the last line the χ^2_{min}-value and the best fit values for our fit-parameters are given.

For the fit where we assume a heavier Higgs-like particle, the χ^2_{min} value improves slightly compared to the one in Figure 5.1 to

$$\chi^2_{min} = 14.1726 \quad \text{at} \quad \langle p\Lambda \rangle = 3.785 \text{ TeV} , \text{ and } \langle \kappa_1 \rangle = 0 \qquad (5.17)$$

The allowed parameter space on 95% confidence-level for the fits with $m_H = 800$ GeV and $m_H = 1.5$ TeV is shown in Figure 5.2.

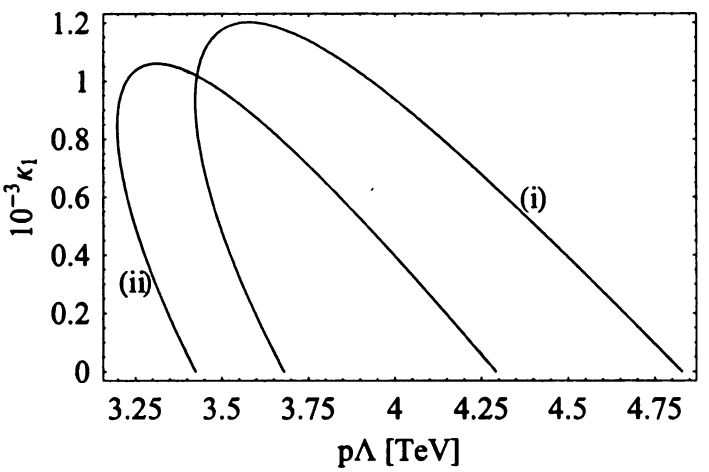

Figure 5.2. The plot shows the allowed region on 95% confidence-level after fitting to the data listed in Figure 5.1. Curve (i) and (ii) enclose the allowed parameter space for $m_H = 800$ GeV and $m_H = 1.5$ TeV respectively.

From Figure 5.2 we can see that the results do not depend significantly on the mass of the Higgs-like particle. Therefore we will assume in the following analysis the Higgs-like particle to have a mass of 800 GeV.

The value for χ^2_{min} being only slightly larger than the number of degrees of freedom $(= 13 - 2)$ tells us that the predictions of our model fit the experimental data well[4]:

$$\chi^2_{min}/\text{d.o.f.} = 1.434.$$

According to Pearson's χ^2-statistic the probability to find χ^2-values greater than this is approximately 15%.

[4]For the standard model with a Higgs mass larger than 800GeV, we estimated $\chi^2_{min} \approx 100$.

The fit gives a lower bound on $p\Lambda$ of about 3.5 TeV and restricts κ_1 to be less than 0.0012. Using the relation from eq.(2.29), we can translate the bounds on the parameter space from Figure 5.2 into the $M_{Z'} - \kappa_1$ plane.

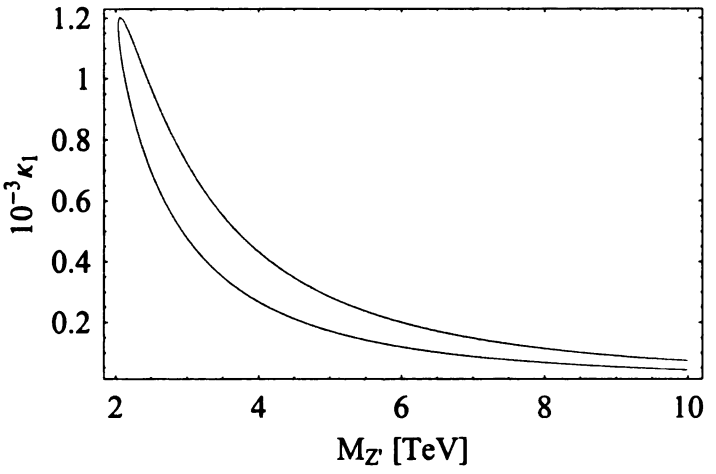

Figure 5.3. The allowed parameter space for $M_{Z'}$ and κ_1.

The plot tells us that we can exclude the Z' to be lighter than 2 TeV on 95% confidence-level. In fact, since the best fit value for κ_1 is zero, it is likely that the Z' is very heavy.

In order to find an estimate for the top-gluon mass, we translate this constraint back into the $\kappa_3 - \kappa_1$ plane, where we encounter a dependence on the hypercharge p of the condensate driving the first symmetry breaking. Since we expect p to be of order one (by comparison with the hypercharges of the familiar particles), the constraints are plotted for $p = \frac{1}{2}$, 1, 2 below, in order to demonstrate how the choice of p affects the evaluation.

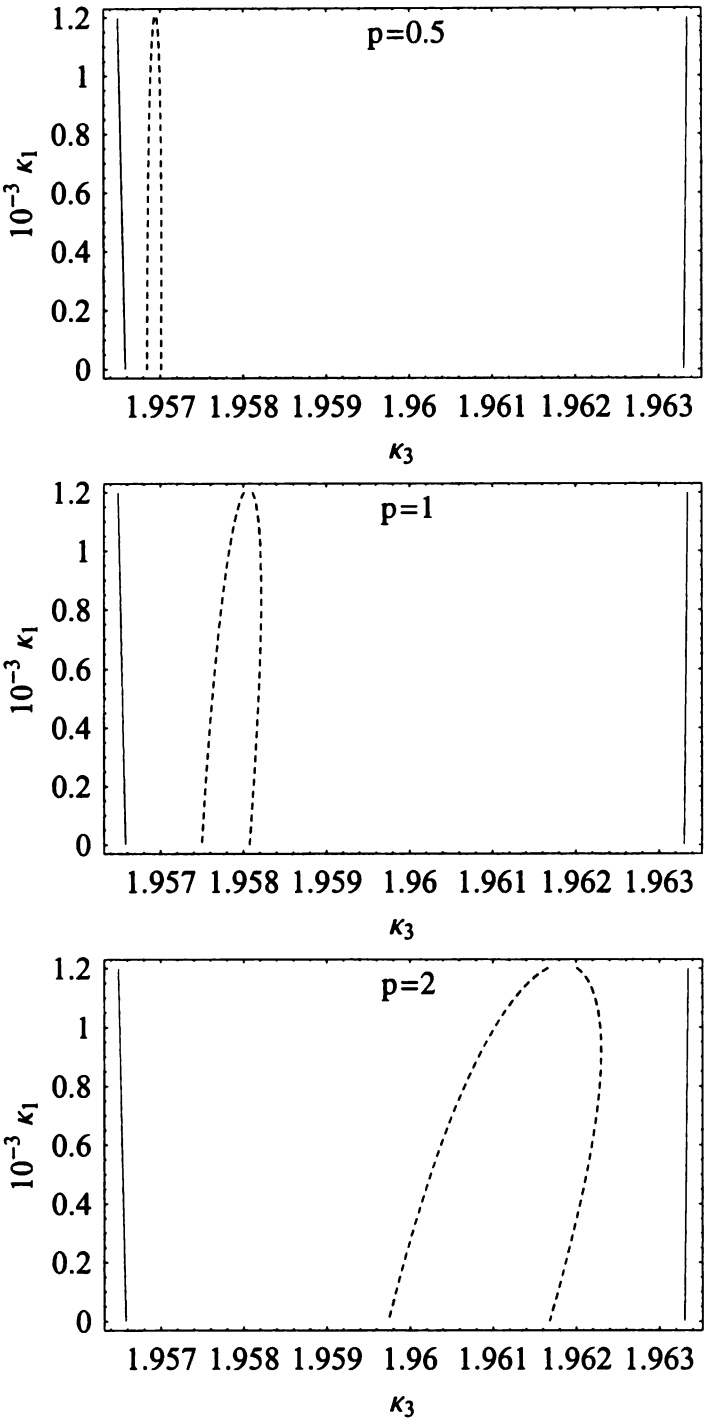

Figure 5.4. The dashed curve encloses the allowed parameter space in the κ_3-κ_1 plane for different values of p. The bold lines represent the tip of the gap triangle (see Fig.3.1).

For small values of p the parameter space becomes extremely narrow and approaches

the line that represents the limit of top-condensation occuring at an infinite scale Λ. This is because small p corresponds to a large top gluon mass. On the other end, large values for p drive the allowed parameter space into a region where, according to the NJL-approximation, b-condensation can occur. Regardless of the exact choice of p, as long as it is of the order of one, we obtain $\kappa_3 \approx 1.96$. Inserting this in eq.(2.29), we find, that the top gluon mass is limited by

$$15 \text{ TeV} \leq M_C \leq 26 \text{ TeV}. \tag{5.18}$$

Even though the estimation of κ_3 requires the NJL-approximation to hold to a (perhaps unreasonably) high accuracy, the general statement that κ_3 (a) has to be large compared to α_S in order to insure top-condensation and is (b) on the other hand restricted not to exceed a certain value to avoid $\langle \bar{b}b \rangle \neq 0$ has to hold, in order to satisfy the general ansatz of our model. Together with the claim of $p \approx 1$, this always yields upper and lower bounds on M_C in analogy to eq.(5.18).

$\mathcal{O}^i$	Zfit ($m_H = 800$GeV)	Zfit ($m_H = 1500$GeV)
Γ_Z [GeV]	2.488069	2.485958
σ_{had} [nb]	41.4881	41.4887
R_e	20.715	20.7118
R_μ	20.715	20.7121
R_τ	20.715	20.7589
A^e_{FB}	0.01444	0.01411
A^μ_{FB}	0.01444	0.0144
A^τ_{FB}	0.01444	0.0144
A^e_{LR}	0.1388	0.1372
A^μ_{LR}	0.1388	0.1372
A^τ_{LR}	0.1388	0.1372
R_b	0.2158	0.2159
R_c	0.1722	0.1722
A^b_{LR}	0.9340	0.9340
A^c_{LR}	0.6642	0.6635
M_W [GeV]	80.23222	80.20047

Table 5.2. shows the best-fit one-loop predictions of the standard model for the set of observables that we used to perform our fit to calculated by ZFITTER for different Higgs masses.

	Γ_Z	$\sigma_{\rm had}$	R_ℓ	A_{FB}^ℓ
Γ_Z	1.000			
$\sigma_{\rm had}$	-0.297	1.000		
R_l	0.004	0.183	1.000	
A_{FB}^l	0.003	0.006	-0.056	1.000

	R_b	R_c	A_{FB}^b	A_{FB}^c	A_{LR}^b	A_{LR}^c
R_b	1.00					
R_c	-0.18	1.00				
A_{FB}^b	-0.10	0.04	1.00			
A_{FB}^c	0.07	-0.06	0.15	1.00		
A_{LR}^b	-0.08	0.04	0.06	-0.02	1.00	
A_{LR}^c	0.04	-0.06	0.01	0.04	0.11	1.00

Table 5.3. Correlation matrices from [7] for the experimental values in Figure 5.1 .

5.2 A fit to a larger set of observables

Barbieri *et al.* [2] have performed a fit to high energy precision data from the LEP1 and LEP2 experiments as well as low energy precision data, like atomic parity violation in Cs atoms.

In the following we use their results to impose bounds on our parameter space and compare it to our results from the previous section. In order to do so, we first have to find a translation for our parametrization into their language.

5.2.1 Definition of electroweak parameters

The standard model predictions at tree-level fit the electroweak precision measurements already very well, so that one expects the effects from beyond the standard model physics to be maximally of the order of the standard model one-loop predictions.

Both the corrections to the standard model one-loop contributions due to new physics (new fermions loops, for example), as well as the deviations from the standard model predictions arising from a whole class of "universal" models at tree-level, can be parametrized in terms of four parameters. Universal, in this context, denotes theories in which the corrections to the standard model predictions can be expressed solely by modifications to the two-point correlation functions of electroweak gauge currents of fermions. Using the parametrization given in [5], the matrix element for the neutral

weak current is given by

$$-M_{NC} = e^2\frac{QQ'}{P^2} + \frac{(T_3 - s^2Q)(T_3' - s^2Q')}{\left(\frac{s^2c^2}{e^2} - \frac{S}{16\pi}\right) + \frac{1}{4\sqrt{2}G_F}\left(1 - \alpha T + \frac{\alpha\delta}{4s^2c^2}\right)}$$
$$+ \sqrt{2}G_F\frac{\alpha\delta}{s^2c^2}T_3T_3' + 4\sqrt{2}G_F(\Delta\rho - \alpha T)(Q - T_3)(Q' - T_3') \qquad (5.19)$$

and the matrix element of the charged current reads

$$-M_{CC} = \frac{(T_+T_-' + T_-T_+')/2}{\left(\frac{s^2}{e^2} - \frac{S}{16\pi}\right)P^2 + \frac{1}{4\sqrt{2}G_F}\left(1 + \frac{\alpha\delta}{4s^2c^2}\right)} + \sqrt{2}G_F\frac{\alpha\delta}{s^2c^2}\frac{(T_+T_-' + T_-T_+')}{2}. \qquad (5.20)$$

P^2 denotes the Euclidean four-momentum transfer, $P^2 = -q^2$, where q is the usual Minkowski momentum. $\Delta\rho$ corresponds to the deviation from unity of the ratio of the strengths of isotriplet weak neutral current and charged current scattering at zero momentum transfer ($P = 0$). The factors $\alpha\delta$ and $(\Delta\rho - \alpha T)$ correspond to the strength of effective contact interactions via extra heavy gauge bosons (from additional $SU(2)$ or $U(1)$ gauge groups). S and T are the parameters from the STU-formalism [16] introduced by Peskin and Takeuchi to characterize the so called "oblige" corrections, i.e. the corrections at one-loop level to the self energies of the standard model gauge bosons due to new physics. s^2 denotes the weak mixing angle as defined by the on-shell Z coupling to the fermions.[5]

The parametrization is chosen such that for the standard model all parameters are zero. Since the standard model predictions are in good agreement with current experiments, one can assume the values of the parameters to be very small compared to one.

In order to find the expressions for the electroweak parameters in our model, we com-

[5]It is, besides eq.(2.51) and(2.53) a fourth possibility to define a weak mixing angle, such that in the standard model at tree level: $s^2 = \sin\theta_W = \sin\theta_Z = \sin\theta$.

pare eq.(5.19) and(5.20) to the respective matrix elements, that we obtain from our model at tree level

$$
\begin{aligned}
-M_{NC} &= e^2\frac{QQ'}{P^2} + \frac{g_Z^2}{P^2-M_Z} + \frac{g_{Z'}^2}{M_{Z'}} \\
&= e^2\frac{QQ'}{P^2} + \frac{e^2}{\sin^2\theta\cos^2\theta}\left[1+\frac{v^2}{p^2\Lambda^2}\cos^2\phi\left(\sin^2\phi-\frac{f_t^2}{v^2}\right)\right]^2 \\
&\quad\times\frac{\left(T_3-Q\left[\sin^2\theta-\frac{v^2}{p^2\Lambda^2}\cos^2\theta\cos^2\phi\left(\frac{f_t^2}{v^2}-\sin^2\phi\right)\right]\right)^2}{P^2+\frac{e^2v^2}{4\cos^2\theta\sin^2\theta}\left(1-\frac{v^2}{p^2\Lambda^2}\left(\sin^2\phi-\frac{f_t^2}{v^2}\right)\right)} \\
&\quad+\frac{\frac{e^2}{cos^2\theta}\cot^2\phi}{\frac{e^2\Lambda^2}{4\cos^2\theta\sin^2\phi\cos^2\phi}}\left(Q-T_3\right)\left(Q'-T_3'\right) \\
&=e^2\frac{QQ'}{P^2}+\frac{\left(T_3-Q\left[\sin^2\theta-\frac{v^2}{p^2\Lambda^2}\cos^2\theta\cos^2\phi\left(\frac{f_t^2}{v^2}-\sin^2\phi\right)\right]\right)^2}{\frac{\sin^2\theta\cos^2\theta}{e^2}\left[1+2\frac{v^2}{p^2\Lambda^2}\cos^2\phi\left(\frac{f_t^2}{v^2}-\sin^2\phi\right)\right]P^2+(M_Z^*)^2} \\
&\quad+\frac{4}{p^2\Lambda^2}\cos^4\phi\left(Q-T_3\right)\left(Q'-T_3'\right), \qquad (5.21)
\end{aligned}
$$

where the contribution of the heavy Z' appears as a contact interaction, assuming $(P^2 \ll M_{Z'})$. The factor in the second line has been pulled out in order to give the numerator the shape of the corresponding term in eq.(5.19). In the next step, its inverse appears to second order in v/Λ in the denominator. $(M_Z^*)^2$ is given by

$$
(M_Z^*)^2 = \frac{v^2}{4}\left[1-\frac{v^2}{p^2\Lambda^2}\left(\frac{F_{TC}^4}{v^2}-\cos^4\phi\right)\right]. \qquad (5.22)
$$

Analogously, we obtain for the charged current

$$
-M_{CC} = \frac{\frac{1}{2}\left(T_+T_-'T_+'T_-\right)}{\frac{\sin^2\theta}{e^2}P^2-\frac{e^2v^2}{4\sin^2\theta}} \qquad (5.23)
$$

From here, we can straightforwardly derive the electroweak parameters in terms of the free parameters of our model [6], by comparing the coefficients in eq.(5.19) and

eq.(5.20) with those from eq.(5.21) and eq.(5.23). At first we express s^2 in terms of our parametrization

$$s^2 = \sin^2\theta + \left(\frac{v}{p\Lambda}\right)^2 \left(\sin^2\phi - \frac{f_t^2}{v^2}\right) \cos^2\phi \cos^2\theta. \tag{5.24}$$

Then, we find

$$\boxed{\frac{\alpha\delta}{4s^2c^2} = 0}, \tag{5.25}$$

since there is no contact interaction term in eq.(5.21) proportional to $T_3 T_3'$. Further

$$\frac{1}{4\sqrt{2}G_F}(1-\alpha T) = \frac{v^2}{4}(1-\alpha T) = \frac{v^2}{4}\left[1 - \frac{v^2}{p^2\Lambda^2}\left(\frac{F_{TC}^4}{v^2} - \cos^4\phi\right)\right]$$

$$\Leftrightarrow \boxed{\alpha T = \frac{v^2}{p^2\Lambda^2}\left(\frac{F_{TC}^4}{v^4} - \cos^4\phi\right)}. \tag{5.26}$$

Here we have used $\sqrt{2}G_F \approx 1/v^2$. Comparing the term in the propagators of the standard model gauge bosons proportional to P^2 yields

$$\boxed{\alpha S = 4\frac{v^2}{p^2\Lambda^2}\cos^2\theta\,\cos^2\phi\left(\sin^2\phi - \frac{f_t^2}{v^2}\right)}. \tag{5.27}$$

From the Z'-term, we obtain

$$\boxed{(\Delta\rho - \alpha T) = \frac{v^2}{p^2\Lambda^2}\cos^4\phi}. \tag{5.28}$$

$\Delta\rho$ is defined by the ratio of the couplings of the $T_3 T_3'$ terms in eq.(5.19) to that of the $(T_+T_-' + T_+'T_-)/2$ term in eq.(5.20). Of course it can also be obtained, by combining eqns.(5.26) and (5.28). Either way yields

$$\boxed{\Delta\rho = \frac{v^2}{p^2\Lambda^2}\frac{F_{TC}^4}{v^4}}. \tag{5.29}$$

The top-gluon sector also shifts the ρ parameter. The main contribution arises from single top gluon exchange across the top and bottom quark loops of W and Z vacuum

polarization diagrams. According to [17] this contribution is given by[6]

$$\Delta\rho^{(C)} \approx \frac{16\pi^2\alpha_Y}{3\sin^2\theta_w}\left(\frac{f_t^2}{M_C M_Z}\right)^2 \kappa_3, \tag{5.30}$$

where M_C denotes the top gluon mass and $\sin\theta_w$ denotes some weak mixing angle, which we set equal to $\sin\theta_Z$[7]. In Figure 5.5, the ratio of the two contributions to $\Delta\rho$ from eq.(5.29) and (5.30) are plotted over the relevant energy regime.

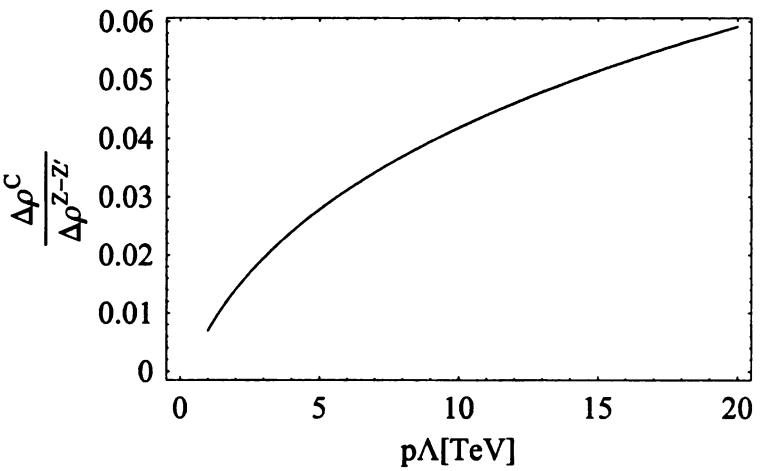

Figure 5.5. The ratio of the two contributions to the ρ-parameter arising from the top gluon and the electroweak sector.

Evidently, the contributions from the top-gluon sector are very small and can be safely neglected in the following.

5.2.2 Constraints from the global fit

At first, I shall briefly outline what the results from [2] that we used to constrain our parameter space correspond to.

The first step of the general fitting procedure closely follows the steps outlined in the

[6]The model [17] has a flavor-universal top gluon-sector, but the couplings of the top gluon to the third generation of fermions are the same in both models.

[7]$\Delta\rho$ is already at the order of $(v/p\Lambda)^2$. Since we are working only to that order in general, the different expressions for the weak mixing angle are equal to each other.

beginning of Chapter 5: For a fit with r parameters to n observables, one first expresses all observables in terms of the chosen parametrization $\theta = (\theta_1, ..., \theta_r)$, yielding terms of the form of eq.(5.1). Since all the parameters are expected to be close to zero, the expressions for the observables are expanded to linear order in θ. Then, the standard model tree-level predictions are replaced by the best fit one-loop prediction of the standard model, which depends on the Higgs mass. This ensures that our parametrization just describes the effect of the new physics.

In the next step, a least-square fit is performed, by minimizing

$$\chi^2(\theta) = \sum_{i,j=1}^{n} \left(\mathcal{O}^i_{exp} - \mathcal{O}^i_{th}(\theta)\right) \left(V^{-1}\right)^{ij} \left(\mathcal{O}^j_{exp} - \mathcal{O}^j_{th}(\theta)\right), \tag{5.31}$$

where $V^{ij} = \sigma^{ik}\rho^{kl}\sigma^{lj}$, with the correlation matrix ρ of the observables and their error matrix σ. Since all $\mathcal{O}^i(\theta)$ are linear in θ, $\Delta\chi^2(\theta) = \chi^2(\theta) - \chi^2_{min}$ is a quadratic form in θ which can be rewritten as

$$\Delta\chi^2(\theta) = \sum_{i,j=1}^{r} \left(\langle\theta^i\rangle - \theta^i\right) \left(U^{-1}\right)^{ij} \left(\langle\theta^j\rangle - \theta^j\right), \tag{5.32}$$

with $U = \sigma\rho\sigma$ denoting the covariance matrix of the best-fit values. This is the desired expression, containing the best-fit value $\langle\theta\rangle$, the standard deviation σ and correlation ρ for the fit parameters.[8]

In order to use the constraints on the electroweak parameters from the global fit performed by Barbieri *et al* [2], we have to express the parameters they used in terms

[8]The division of $U = \sigma\rho\sigma$ is unique, since the correlation matrix ρ is defined to have diagonal entries of 1.

of our parametrization. According to [5], the Barbieri parameters read in our basis

$$\hat{S} \equiv \frac{1}{4s^2}\left(\alpha S + 4c^2\left(\Delta\rho - \alpha T\right)\right) + \frac{\alpha\delta}{c^2} = \frac{v^2}{p^2\Lambda^2}\frac{c^2}{s^2}\frac{F_{TC}^2}{v^2}\cos^2\phi \tag{5.33}$$

$$\hat{T} \equiv \delta\rho = \frac{v^2}{p^2\Lambda^2}\frac{F_{TC}^2}{v^2} \tag{5.34}$$

$$Y \equiv \frac{c^2}{s^2}\left(\Delta\rho - \alpha T\right) = \frac{v^2}{p^2\Lambda^2}\frac{c^2}{s^2}\cos^4\phi \tag{5.35}$$

$$W \equiv \frac{\alpha\delta}{4s^2c^2} = 0 \tag{5.36}$$

The constraints on those parameters obtained from the fit are listed in Table 5.4.

$m_H[GeV]$	$10^3\langle\hat{S}\rangle$	$10^3\langle\hat{T}\rangle$	$10^3\langle Y\rangle$	$10^3\langle W\rangle$
800	-0.9 ± 1.3	2.0 ± 1.0	0.0 ± 1.2	-0.2 ± 0.8

Table 5.4. The values for the electroweak parameters obtained from a global fit to LEP1 and LEP2 data, according to [2].

The corresponding correlation matrix, regardless of the Higgs mass, given in [2] is

$$\rho = \begin{pmatrix} 1 & 0.68 & 0.65 & -0.12 \\ 0.68 & 1 & 0.11 & 0.19 \\ 0.65 & 0.11 & 1 & -0.59 \\ -0.12 & 0.19 & -0.59 & 1 \end{pmatrix} \tag{5.37}$$

Since we only have two free parameters in our model $\Delta\chi^2$ is not zero for the best-fit values of our parameters. The allowed parameter space at 95% (2σ)-confidence level is obtained by requring

$$6.17 + \Delta\chi^2(\langle p\Lambda\rangle, \langle\kappa_1\rangle) \geq \begin{pmatrix} \langle\hat{S}\rangle - \hat{S} \\ \langle\hat{T}\rangle - \hat{T} \\ \langle Y\rangle - Y \\ \langle W\rangle - W \end{pmatrix}^T (\sigma\,\rho\,\sigma)^{-1} \begin{pmatrix} \langle\hat{S}\rangle - \hat{S} \\ \langle\hat{T}\rangle - \hat{T} \\ \langle Y\rangle - Y \\ \langle W\rangle - W \end{pmatrix}, \tag{5.38}$$

with $\sigma = \mathrm{diag}\left(\sigma\hat{S}, \sigma\hat{T}, \sigma Y, \sigma W\right)$. Inserting eqns.(5.33)-(5.36) and the values from Table 5.4, yields the bounds on the parameter space shown in Figure 5.6:

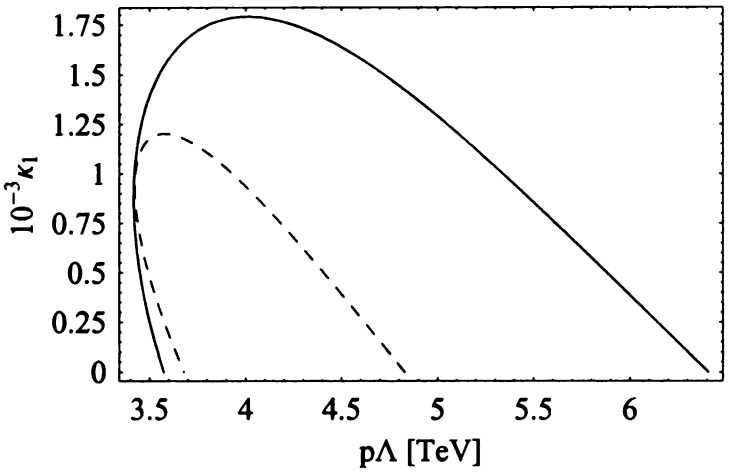

Figure 5.6. The constraints on the parameter space of our model from a fit to LEP1 and LEP2 data [2] under the assumption of a Higgs mass of 800 GeV. The dashed line shows the result from our fit in the previous section for comparison.

Surprisingly the parameter space becomes wider if one takes more data into account. In [2] there is unfortunately neither a χ^2_{min} value nor the pulls for the observables given which limits our possibilities to understand this. There has to be a tendency among the extra observables to pull the best fit value for $p\Lambda$ toward larger values. The lower limit on $p\Lambda$ remains the same, so that the lower bound on $M_{Z'}$ does not shift.

Chapter 6

Summary and Conclusions

6.1 Summary of the Results

Based on the fits to electroweak precision data, we can exclude on 95% confidence-level Z' masses below 2 TeV. With the upper bound on its coupling to fermions ($\kappa_1 \leq 0.0015$), this tells us that our model does not get in conflict with the bounds on effective four-fermion interactions from the LEP2 measurements (see section 4.2). The strong upper bound on κ_1 also ensures that, in the sense of our results from the calculation of the Landau-pole (section 3.2), our theory can (technically) be valid up to scales beyond the Planck-scale.

Given the analysis in section 4.1 and the estimation of the topgluon mass in eq.(5.18), we do not expect our model to give rise to flavor changing neutral currents in a detectable range.

For further investigation of this model it may be useful to express our results in terms of the universal parameters S, T, and $\Delta\rho$ from eq.(5.26) through (5.29):

$$\Delta\rho = \alpha T = 2.9 \times 10^{-3} \quad \text{and} \quad \alpha S = 0. \tag{6.1}$$

From here we see that we are basically left with one free parameter, because $\kappa_1 \to 0$. Looking back at eq.(3.3), we find that the "tilting" that makes the top quark form a condensate but not the bottom quark is dominated by the unbroken electroweak gauge interactions. The exchange of a heavy Z' boson hardly affects the tilting process ($\kappa_1 \ll \alpha_Y$). This forces κ_3 to be "fine-tuned" in the sense that it has to be very close to the critical coupling at which a condensation of third generation quarks occurs. This corresponds to the very narrow parameter space in the $\kappa_3 - \kappa_1$ plane as shown in Figure 5.4.[1]

This leaves us with a "sterile" Z' boson which in a good approximation does not couple to fermions at all. Nonetheless it is a key ingredient in the model, since the goodness of our fit relies on its contribution to the shift in the coupling of the ordinary Z boson to fermions:

$$\lim_{\kappa_1 \to 0} g_Z^f = \left(T_3 - \sin^2\theta_Z\right) + \left(\frac{v}{p\Lambda}\right)^2 \left(1 - \frac{f_t^2}{v^2}\right) \frac{\cos^2\theta_Z \sin^2\theta_Z}{\cos^2\theta_Z - \sin^2\theta_Z} Q\,. \tag{6.2}$$

6.2 Expectations on Future Experiments

The most exciting experiment (not only regarding our model) will evidently be the search for the Higgs-boson at the LHC. If a Higgs-particle with standard model-like couplings to the other particles will be detected, our model, and nearly the entire class of Technicolor models, becomes obsolete.

Apart from this, it is hard to make predictions from our model for possible observations at LHC or ILC, since the masses of the heavy gauge bosons are already, by the current electroweak precision data, forced beyond the reach of those colliders. The Z' is not necessarily very heavy but its coupling to fermions as well as its mixing with

[1]The graphs were obtained using the NJL-approximation, but the statement about the "fine-tuned" parameter κ_3 holds for any possible model describing this pattern of symmetry breaking.

the standard model Z is very small which makes direct searches unrealistic.

From ILC one can expect upper bounds on effective four-quark interactions[2] similar to the LEP2 data that we used in section 4.2. In contrast to the analysis of the Z'-exchange, where $\kappa_1 \to 0$ can compensate for arbitrarily small masses of the Z' boson, κ_3 has to be large compared to α_S in order to provide the desired top-condensation. A strong lower bound on the mass of the top-gluon M_C may, according to eq.(2.29), drive the scale Λ out of the region allowed by electroweak precision data.[3] The general ansatz of explaining the large top-mass via extra dynamics singling out the third generations of fermions, leads to potentially detectable decays of for example top-pions into $b\bar{b}$, but predictions for such processes exceed, unfortunately, the subject of this thesis.

[2]The author would like to thank his advisor Prof. Elizabeth Simmons for pointing this out.

[3]At least under the assumption that the hypercharge of the condensate driving the first symmetry breaking is of order 1.

APPENDIX

APPENDIX A

A.1 Constraints from Electroweak Precision Data on Models with a Flavor Non-Universal Hypercharge Sector

Flavor non-universal topcolor models (as in [17]) usually assume that the third generation of fermions transforms under the $U(1)_1$ group and first and second generations under the $U(1)_2$ group (see Table 2.1). Therefore, the Z boson couples differently to the third than to the other fermion generations. This can be seen by looking back at eq.(2.49), where we have used that, in the flavor-universal model, the operator

$$Y_1 - (Y_1 + Y_2)\sin^2\theta = Y\cos^2\theta, \tag{A.1}$$

for all fermions. This relation has to be modified in the flavor non-universal case. For the third generation of fermions the Z boson coupling stays the same as in eq.(2.49), but for the first two generations the coupling takes the form

$$\begin{aligned} g_Z^{1,2} = & \frac{e}{\sin\theta\cos\theta}\left[T_3\left(1-\frac{v^2}{p^2\Lambda^2}\sin^2\phi\left(\sin^2\phi-\frac{f_t^2}{v^2}\right)\right)\right. \\ & \left. - Q\left(\sin^2\theta-\frac{v^2}{p^2\Lambda^2}\sin^2\phi\left(\sin^2\phi-\frac{f_t^2}{v^2}\right)\right)\right] \end{aligned} \tag{A.2}$$

The fitting procedure from the last section can be easily applied to this class of models as well. While calculating the values for observables as predicted by these models, one has to keep track of the couplings of the Z boson. As set of experimental values

we used the same as in the previous section, with the exception that the values for observables depending on the coupling of the Z boson to leptons have to be replaced by those which are given in [7] for the flavor non-universal case.

We have only performed this fit assuming a Higgs-like particle of mass $m_H = 800$ GeV. The result of our fit and the experimental values are given in Figure A.1. The additional correlation matrices to Table 5.3 are given in Table A.1 and A.2.

Experimental Value	Fit	Pull
Γ_Z= (2.4952±0.0023) GeV	2.4892 GeV	
σ_{had}= (41.541±0.037) nb	41.4598 nb	
R_e= 20.804±0.050	20.7428	
R_μ= 20.785±0.033	20.7431	
R_τ= 20.764±0.045	20.7515	
A^s_{FB}= 0.0145±0.0025	0.01682	
A^μ_{FB}= 0.0169±0.0013	0.01682	
A^τ_{FB}= 0.0188±0.0017	0.0160	
A^τ_{LR}= 0.1465±0.0033	0.1417	
A^s_{LR}(SLD)= 0.1516±0.0021	0.1493	
A^μ_{LR}(SLD)= 0.142±0.015	0.1493	
A^τ_{LR}(SLD)= 0.136±0.015	0.1417	
R_b= 0.21629±0.00066	0.2160	
R_c= 0.1721±0.0030	0.1722	
A^b_{FB}= 0.0992±0.0016	0.1046	
A^c_{FB}= 0.0707±0.0035	0.07454	
A^b_{LR}= 0.923±0.020	0.9342	
A^c_{LR}= 0.670±0.027	0.6688	
M_W= (80.403±0.029) GeV	80.2970 GeV	
		0 1 2 3
χ^2_{min}=49.9627	at $\langle p\Lambda \rangle$ = 6.629 TeV, $\langle \kappa_l \rangle$ = 0	

Figure A.1. The first column shows experimental values from [7] for the set of observables we used to fit the predictions of our model to. In the second column the best-fit results for our model are listed and the graph on the right-hand side shows the pulls for each observable. In the last line the χ^2_{min}-value and the best fit values for our fit-parameters are given.

The χ^2_{min}-value in this case is large which makes the it unlikely that a model like this fits the data well. Comparing the pulls in this case to Figure 5.1, one can see that the agreement of the predicted values with the experimental data is not as good as

for the flavor-universal model.

From the analysis of the flavor universal case, we have seen that $\kappa_1 = \alpha_Y \cot^2\phi$ has to be very small in order to fit the data well. In the flavor non-universal model this corresponds to make the shift compared to the standard model coupling in the Z coupling to third generation small. At the same time this shift becomes large in the coupling to the first two fermion generations which spoils the fit. Therefore one might expect the best fit value for κ_1 to be positive which is not the case. One has to take into account that the coupling of the Z boson contains a flavor-independent dependency on κ_1 due to the shift in the weak mixing angle in eq.(2.52). Obviously, this contribution primarily has to be zero in order to fit the data.[1] The "allowed" parameter space is shown in Figure A.2, but since the χ^2_{min}-value is so large the meaning of this becomes ambiguous.

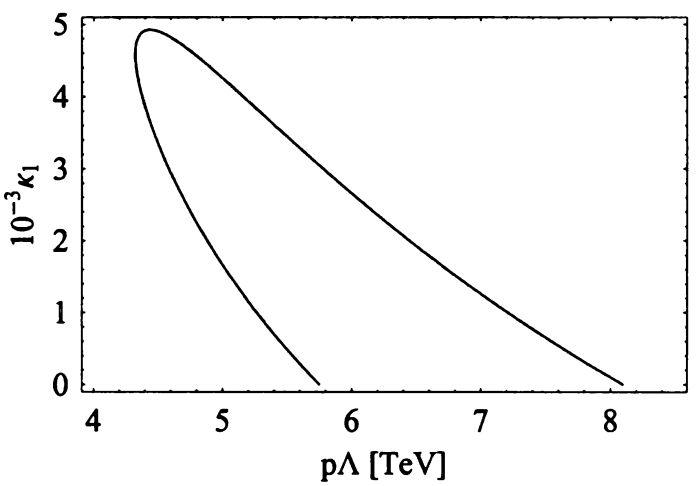

Figure A.2. The plot shows the allowed parameter space on 95% confidence-level for a flavor non-universal model after fitting to electroweak precision data [7].

Generally speaking, one can conclude that model with a flavor non-universal hypercharge sector are disfavored by the current electroweak precision data.

[1] I double-checked this by interchanging the couplings of the third generation with the couplings of the first two fermion generations to the Z boson.

	Γ_Z	$\sigma_{\rm had}$	R_e	R_μ	R_τ	A_{FB}^e	A_{FB}^μ	A_{FB}^τ
Γ_Z	1.000							
$\sigma_{\rm had}$	-0.297	1.000						
R_e	0.011	0.105	1.000					
R_μ	0.008	0.131	0.069	1.000				
R_τ	0.006	0.092	0.046	0.069	1.000			
A_{FB}^e	0.003	0.001	-0.371	0.001	0.003	1.000		
A_{FB}^μ	0.002	0.003	0.020	0.012	0.001	-0.024	1.000	
A_{FB}^τ	0.001	0.002	0.013	-0.003	0.009	-0.020	0.046	1.000

Table A.1. The correlation matrix of the experimental values for the flavor non-universal case.

	A_{LR}^e	A_{LR}^μ	A_{LR}^τ
A_{LR}^e	1.000		
A_{LR}^μ	0.038	1.000	
A_{FB}^ℓ	0.033	0.007	1.000

Table A.2. The submatrix for the correlations of the lepton left-right asymmetries.

BIBLIOGRAPHY

BIBLIOGRAPHY

[1] A. B. Arbuzov, M. Awramik, M. Czakon, A. Freitas, M. W. Gruenewald, K. Moenig, S. Riemann, and T. Riemann. Zfitter: a semi-analytical program for fermion pair production in e+e- annihilation, from version 6.21 to version 6.42, 2006.

[2] Riccardo Barbieri, Alex Pomarol, Riccardo Rattazzi, and Alessandro Strumia. Electroweak symmetry breaking after lep1 and lep2. *Nuclear Physics B*, 703:127, 2004.

[3] Ta-Pei Cheng and Ling-Fong Li. *Gauge Theory of Elementary Particle Physics.* Oxford Press, 2005.

[4] R. S. Chivukula and J. Terning. Precision electroweak constraints on top-color assisted technicolor. *Physics Letters B*, 385:209, 1996.

[5] R. Sekhar Chivukula, Hong-Jian He, Masafumi Kurachi, Elizabeth H. Simmons, and Masaharu Tanabashi. Universal non-oblique corrections in higgsless models and beyond. *Physics Letters B*, 603:210, 2004.

[6] R.Sekhar Chivukula and Elisabeth H.Simmons. Elecktroweak parameters in $SU(2) \times U(1)^2$ triangle moose. March 22 2007.

[7] The ALEPH Collaboration, The DELPHI Collaboration, the L3 Collaboration, The OPAL collaboration, The SLD Collaboration, the LEP Electroweak Working Group, the SLD Electroweak, and Heavy Flavour Groups. Precision electroweak measurements on the z resonance. *Physics Reports*, 427:257, 2006.

[8] Yao et al. Review of particle physics, 2006.

[9] E. Farhi. An introduction to symmetry breaking in the standard model. Prepared for Theoretical Advanced Study Institute in Elementary Particle Physics (TASI 91): Perspectives in the Standard Model, Boulder, CO, 2-28 Jun 1991.

[10] Edward Farhi and Leonard Susskind. Technicolor. *Phys. Rept.*, 74:277, 1981.

[11] Christopher T. Hill. Topcolor assisted technicolor. *Physics Letters B*, 345:483, 1995.

[12] Christopher T. Hill and Elizabeth H. Simmons. Strong dynamics and electroweak symmetry breaking. *Phys. Rept.*, 381:235–402, 2003.

[13] Bob Holdom. Raising the sideways scale. *Phys. Rev.*, D24:1441, 1981.

[14] S. Kirsch and T. Riemann. Smatasy - a program for the model independent description of the z resonance. *Computer Physics Communications*, 88:89, 1995.

[15] Michael E. Peskin and D. V. Schroeder. An introduction to quantum field theory. Reading, USA: Addison-Wesley (1995) 842 p.

[16] Michael E. Peskin and Tatsu Takeuchi. New constraint on a strongly interacting higgs sector. *Phys. Rev. Lett.*, 65(8):964–967, Aug 1990.

[17] Marko B. Popovic and Elizabeth H. Simmons. A heavy top quark from flavor-universal colorons. *Physical Review D*, 58:095007, 1998.

[18] Chris Quigg. Introduction to gauge theories of the strong, weak, and electromagnetic interactions. *NATO Adv. Study Inst. Ser. B Phys.*, 66:143, 1980.

[19] J. Terning. Modern supersymmetry: Dynamics and duality. Oxford, UK: Clarendon (2006) 324 p.